

1
2
3
4
5
6
7
8
9
10
11
12
13
14
15
16
17
18
19
20
21
22
23
24
25
26
27

Kinematic constraints on the Rodinia-Gondwana transition

Andrew S. Merdith^{*1,2}, Simon E. Williams¹, R. Dietmar Müller¹, Alan. S. Collins³

* Corresponding author: Andrew.merdith@sydney.edu.au

¹ EarthByte Group, School of Geosciences, The University of Sydney, Madsen Building F09, Australia

² Data61, Australian Technology Park, Australia

³ Tectonics, Resources and Exploration (TRaX), Department of Earth Science, The University of Adelaide,
SA 5005, Australia

Key words: kinematic; Neoproterozoic, Gondwana amalgamation, Rodinia breakup, plate tectonics

28 **Abstract**

29

30 Earth's plate tectonic history during the breakup of the supercontinent Pangea is well constrained from the
31 seafloor spreading record, but evolving plate configurations during older supercontinent cycles are much less
32 well understood. A relative paucity of available paleomagnetic and geological data for deep time
33 reconstructions necessitates geoscientists to find innovative approaches to help discriminate between
34 competing plate configurations. Periods of supercontinent assembly may be better constrained where
35 paleomagnetic and geological data from multiple continental blocks can be combined. More difficult is tracing
36 the journeys of individual continents during the amalgamation and breakup of supercontinents. Typically
37 deep-time reconstructions are built using absolute motions defined by paleomagnetic data, and do not consider
38 the kinematics of relative motions between plates, even for occasions where they are thought to be 'plate-
39 pairs', either rifting apart leading to the formation of conjugate passive margins separated by a new ocean
40 basin, or brought together by collision and orogenesis. Here, we use open-source software tools
41 (GPlates/pyGPlates) that allow geoscientists to easily access quantitative plate kinematics inherent within
42 alternative reconstructions, such as rates of absolute and relative plate motion. We analyse the Rodinia-
43 Gondwana transition during the Neoproterozoic, investigating the proposed Australia-Laurentia
44 configurations during Rodinia, and the motion of India colliding with Gondwana. We find that earlier rifting
45 times provide more optimal kinematic results. The AUSWUS and AUSMEX configurations with rifting at
46 800 Ma are the most kinematically supported configurations for Australia and Laurentia (average rates of 57
47 and 64 mm/yr respectively), and angular rotation of $\sim 1.4^\circ/\text{Myr}$, compared to a SWEAT configuration
48 (average spreading rate ~ 76 mm/yr) and Missing-Link configuration (~ 90 mm/yr). Later rifting, at 725 Ma
49 necessitates unreasonably high spreading rates of >130 mm/yr for AUSWUS and AUSMEX and ~ 150
50 mm/yr for SWEAT and Missing-Link. Using motion paths and convergence rates, we create a kinematically
51 reasonable (convergence below 70 mm/yr) tectonic model that is built upon a front-on collision of India into
52 Gondwana, while also incorporating a sinistral strike-slip motion against Australia and East Antarctica. We
53 use this simple tectonic model to refine a global model for the break-up of western Rodinia and the transition
54 to eastern Gondwana. Our refined tectonic model for the Neoproterozoic, beginning with the breakup of the

55 supercontinent Rodinia, provides an improved paleogeographic basis for investigating the causes of major
56 climate change and the subsequent evolution of complex life.

57

58 **Introduction**

59

60 Our knowledge of plate tectonic configurations through Earth history is limited by the availability of
61 geoscientific data through time and space. Geological, geophysical, paleomagnetic, geochemical, structural
62 and tectonic (e.g. large scale orogenies, passive margins) information helps to constrain both the motions of
63 plates, and the relative configurations of continents within past supercontinents. The fabric and geophysical
64 signatures preserved within the ocean basins, in particular, magnetic anomalies and fracture zones (Matthews
65 et al. 2011; Wessel and Müller, 2015), allow the construction of detailed, global relative plate models for
66 Mesozoic and Cenozoic times (e.g. Müller et al. 2016; Seton et al. 2012). These features indicate the extent to
67 which relative plate motions are stable or change over timescales of millions to tens-of-millions years. For
68 example, spreading rates globally are typically in the range 10 to 70 mm/yr. In the Atlantic basins, spreading
69 rates have remained within 20 and 40 mm/yr over the last ~200 Myr. Other ocean basins have witnessed
70 much larger variations in spreading rates, and changes in direction of relative plate motion at spreading
71 centres, witnessed by sharp fracture zone bends (Matthews et al, 2011; 2012), notably along spreading centres
72 in the Indian ocean. Mechanisms to explain major changes in relative plate motion rate and direction are
73 either grouped into ‘top-down’ tectonic mechanisms or ‘bottom-up’ mantle flow mechanisms. Tectonic
74 mechanisms relate to changes in plate boundary forces such as subduction initiation (e.g. Whittaker et al.
75 2007), cessation (Austermann et al. 2011, Patriat and Achache, 1984), or changes in the subduction regime
76 through subduction of ridges (Seton et al. 2015), thick oceanic crust (Knesel et al. 2008) or young buoyant
77 oceanic crust (Matthews et al. 2012). Proposed mantle flow mechanisms include plume arrival (Cande and
78 Stegman 2011; van Hinsbergen et al. 2011), decoupling due to lubrication from plume arrival (Ratcliff et al.
79 1998) and heat buildup around subducted slabs leading to a reduction of negative buoyancy (King et al. 2002;
80 Lowman et al. 2003). Feedback mechanisms between orogenesis and changes in convergence rates have also
81 been proposed (e.g. Iaffaldano et al. 2006).

82

83 The supercontinent cycle theory implies that over time continents disperse forming ocean basins, before re-
84 amalgamating into a new supercontinent. Evidence for this is provided by a number of punctuated geological
85 and geochemical secular trends, such as in zircons which act as a proxy for continental magmatism (Belousova
86 et al. 2010), the formation of mineral deposits (Bierlein et al. 2009; Groves et al. 1998; Pehrsson et al. 2016),
87 and large igneous provinces (Bradley 2011; Nance and Murphy 2013). The theory suggests that the formation
88 and breakup of supercontinents are intricately linked to both deeper earth processes, as well as surface, ocean
89 and atmospheric processes (Bradley 2011; Nance et al. 2014). While Pangea, the last supercontinent, is well
90 known, Proterozoic supercontinents are less well established due to the absence of ocean basins and the
91 paucity of fossil evidence. Rodinia is the hypothesised late Mesoproterozoic to early Neoproterozoic
92 supercontinent, originally envisioned on the basis of global orogenies (the Grenvillian orogeny of Laurentia
93 and coeval Stenian-Tonian orogenies worldwide) at ca.1.2-0.9 Ga (Dalziel 1991; Hoffman 1991; Moores
94 1991). However, not all Proterozoic cratons clearly exhibit Stenian-Tonian aged orogenies, even if they do,
95 the orogenies are not synchronous (Fitzsimons 2000), and, as more data have become available, a proliferation
96 of plate configurations for the Neoproterozoic have been developed, including models with a large, long-lived
97 Rodinia (Johansson 2014; Li et al. 2008), paleomagnetically defined models (Evans 2009; Powell et al. 1993),
98 and models that have a partially complete supercontinent, with one-two cratons separate (usually Congo-São
99 Francisco and/or India, e.g. Collins and Pisarevsky 2005; Meert 2003). Generally, most models of Rodinia
100 tend to have Laurentia as the heart of the supercontinent due to the presence of rifted margins on the perimeter
101 of the continent. Australia–East-Antarctica are typically matched to the western coast of Laurentia; Siberia-
102 North China off the northern margin; Amazonia, Baltica and West Africa on the eastern margin; and the
103 Kalahari craton on the southern margin (e.g. Collins and Pisarevsky 2005; Dalziel 1991; Hoffman 1991;
104 Johansson 2014; Li et al. 2008, 2013; Meert and Torsvik 2003; Moores 1991), though some variations exist
105 (e.g. Sears and Price 2003).

106

107

108 For pre-Pangea times, where ocean basins are not preserved, it becomes more important to use other
109 approaches to help discriminate between competing plate motions and continental configurations. Typically
110 either geological or paleomagnetic data (or a combination of both) is used to build deep-time plate models.

111 For example Goodge et al. (2008) used isotopic data from granites to tie East-Antarctica and Laurentia
112 together at ~1.4 Ga, Ganade et al. (2016) dated zircons to constrain the timing of western Gondwana
113 collision, geochemical signatures of large igneous provinces were used to determine pre-rift matches of cratons
114 for Kenorland, Nuna and Rodinia (e.g. Ernst et al. 2008; 2013; Ernst and Bleeker 2010) and detrital zircon
115 analyses have been used to link provenances together (e.g. Li et al. 2015; Mulder et al. 2015; Wang and Zhou
116 2012,) and measure secular changes in volume of continental crust (e.g. Condie et al. 2009; Nance et al. 2014).
117 Evans (2009) constructed a (completely) paleomagnetically derived model of Rodinia, and Meert (2002) built a
118 paleomagnetically constrained model of Nuna. Recent models that integrate both geological and
119 paleomagnetic data for the globe have also been developed for Nuna (Pisarevsky et al. 2014) and Rodinia (Li
120 et al. 2008, 2013). These models anchor relative plate configurations and motions suggested by geology with
121 absolute position as determined through paleomagnetic data, as approaches to determining absolute plate
122 motions for recent times (e.g. hot spot chains (Morgan, 1971; Müller et al. 1993; Steinberger et al. 2004) and
123 tomographic imaging of slabs (Butterworth et al. 2014; van der Meer et al. 2010) are not applicable to deep
124 time reconstructions.

125

126 Absolute plate motion models constructed for the Paleozoic (Domeier 2015; Domeier and Torsvik 2014;) use a
127 combination of paleomagnetic data and large low-shear-velocity provinces (LLSVPs) to constrain
128 paleolatitude and paleolongitude (Torsvik et al. 2008). These models are also supplemented with geological
129 and paleontological data (e.g. Cocks and Torsvik 2002; Torsvik and Cocks 2013) to help with constraining the
130 timing of events, paleolatitude and plate configurations. For all but the latest Neoproterozoic reconstructions,
131 paleontological data are unavailable as complex life had not yet evolved; therefore the focus shifts to either
132 paleomagnetic and/or geological information to reconstruct plate motions. During supercontinent assembly
133 times, paleomagnetic data are especially useful, as a small number of reliable poles from different blocks can
134 be pooled together to constrain the motion of a large number of cratons, leading to models that are grounded
135 with absolute plate motions; however, during times of supercontinent dispersal and amalgamation it becomes
136 more difficult to infer absolute plate motions due to fragmented apparent polar wander paths (APWPs). Two
137 consequences of this are the development of tectonic models that cluster around paleomagnetic ‘pierce points’
138 (i.e. times at which high quality paleomagnetic data exist) such that these models simply consist of a series of

139 snapshots of the positions of continents at specified times without incorporating relative motions suggested by
140 geology, and, secondly, tectonic models that are unable to distinguish between some competing configurations
141 or motions due to missing or poor quality data.

142
143 The Neoproterozoic, in particular the transition to Gondwana from Rodinia, is a key stage in global plate
144 reconstructions due to the (near-)global glaciation events that occurred at that time (e.g. Gernon et al. 2016;
145 Hoffman and Li 2009; Schmidt and Williams 1995) and because many present-day continents were formed
146 during this transition. Gondwana, consisting primarily of Africa, South America, Australia, India and
147 Antarctica, was the precursor to Pangea, and the major landmass of the southern hemisphere for much of the
148 Phanerozoic. It occupies a particularly important position for both geological and biological purposes, as it is
149 the oldest proposed supercontinental amalgamation for which a variety of geological data are readily available
150 (Cawood and Buchan, 2007; Collins and Pisarevsky, 2005; Li et al. 2008; Meert 2003), as well being integral
151 to the evolution and dispersion of complex life (e.g. Brasier et al. 2001; Halverson et al. 2010; Maruyama and
152 Santosh 2008; Meert and Lieberman 2003; Santosh 2010; Squire et al. 2006).

153
154 Here we present an alternative approach to discriminate between competing Proterozoic reconstructions, using
155 kinematic data extracted from a continent-focussed plate reconstruction model (adapted from Li et al. 2008;
156 2013). We use relative plate motion kinematics to help make informed decisions for plate reconstructions
157 during times of supercontinent dispersal and amalgamation, when large gaps in the coverage of paleomagnetic
158 data limit our ability to constrain plate motions. From this, we generate a simple tectonic reconstruction of the
159 breakup of western Rodinia and amalgamation of eastern Gondwana. We demonstrate this during dispersal
160 times by comparing the four competing Neoproterozoic configurations of Laurentia and Australia–East-
161 Antarctica; SWEAT, AUSWUS, AUSMEX and South China as a ‘Missing-Link’ (Fig. 1a-d), reconstructing
162 them from a common end point (650 Ma) back to the possible rifting times permitted by both paleomagnetic
163 and geological data, and then in times of amalgamation, by tracing and constraining the relative motions of
164 India with respect to Australia, and with respect to the Congo-São Francisco continent.

165
166

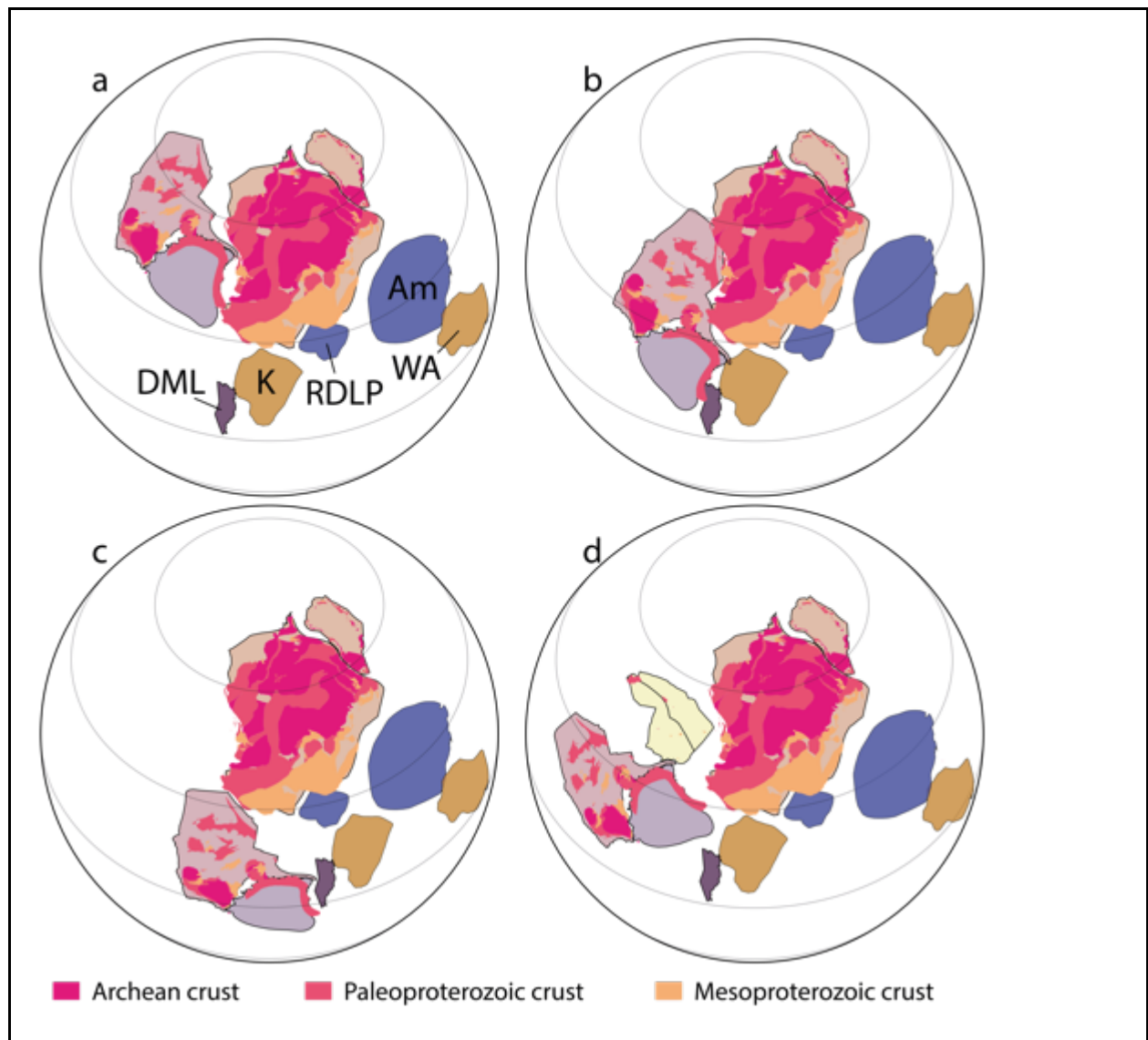


Figure 1: The different configurations of Laurentia with Australia-Eastern Antarctica and South China with pre-Neoproterozoic geology overlain. Laurentia is fixed in its present day position. (a) SWEAT fit, eastern Antarctica is pushed against the southwest US, while Australia lies further north near the US-Canadian border (Dalziel, 1991; Hoffman, 1991; Moores, 1991); (b) AUSWUS fit, eastern Australia is matched against the southwest United States of America (Karlstrom et al. 1999); (c) AUSMEX, Australia has only a small connection with Laurentia, where the north tip of Queensland fits against Mexico (Wingate et al. 2002), Kalahari Craton is shifted further south to accommodate Mawson; (d) Missing-Link model, which fits South China as a continental slither between Australia and Laurentia (Li et al. 1995). Laurentia is rotated to its 800 Ma position (after Li et al. 2008; 2013). Geology is taken from the Geodynamic map of

Rodinia after Li et al. (2008). Am, Amazonia; DML, Dronning Maud Land; K, Kalahari; RDLP, Rio de la Plata; WA, West Africa.

167

168

169 **Methodology**

170

171 We investigate the relative motion for two specific geological episodes: firstly, rifting between Australia—East-
172 Antarctica and Laurentia during Rodinia breakup and subsequent continued divergence; and secondly,
173 convergence between India and Australia, and India and Congo, during Gondwana amalgamation. The rifting
174 time and alternative configurations of Australia—East-Antarctica and Laurentia were analysed to determine
175 which timings and configurations are more kinematically feasible (i.e. at least compared to present-day
176 kinematics) as well as to determine the possible range of relative paleolongitudinal distance between
177 Australia—East-Antarctica and Laurentia for times postdating their interpreted connection. For the
178 amalgamation of eastern Gondwana, known geological and paleomagnetic constraints of India, Congo and
179 Australia were used to build a kinematically feasible, relative plate convergence model. The different
180 scenarios, based on alternative Rodinian configurations, for Australia—East-Antarctica - Laurentia rifting, as
181 well as the geological and paleomagnetic data pertinent to India’s convergence into Gondwana are outlined
182 below.

183

184 **Previous Analysis**

185

186 Four configurations of the Australia—East-Antarctica – Laurentia connection have been proposed in the last
187 twenty years based on geological and paleomagnetic grounds, though both sets of data are insufficient to fully
188 discriminate between them. SWEAT, juxtaposing the south-west USA with eastern Antarctica (Australia lies
189 further north near Wyoming and the Canadian border) (Dalziel 1991; Hoffman 1991; Moores 1991) (Fig. 1a);
190 AUSWUS, which matches the east coast of Australia with the west coast of the USA (Karlstrom et al. 1999)
191 (Fig. 1b); AUSMEX, which pushes Australia—East-Antarctica further south, such that Queensland is against

192 Mexico (Wingate et al. 2002) (Fig. 1c); and the Missing-Link model, which fits South China as a continental
193 slither between Laurentia and Australia (Li et al. 1995) (Fig. 1d).

194

195 Generally, the conjugate margins of both corresponding continents have thick sedimentary sequences intruded
196 by magmatic dykes (e.g. Davidson 2008; Priess 2000; Rainbird et al. 1996; Walter et al. 1994; Young et al
197 1979) that suggest rifting somewhere between 825-700 Ma, though the transition from rift to drift is
198 unconstrained partly due to difficulties in precisely dating many of the formations of the Adelaidian Rift
199 Complex.

200

201 *SWEAT*

202

203 The original Rodinian connection proposed between Laurentia and Australia by Dalziel (1991), Hoffman
204 (1991) and Moores (1991) was based on a number of similarities such as an extension of the Grenvillian
205 Orogeny into Antarctica (and India) (Moores 1991) and similar tectonic histories and tectonostratigraphy of
206 their margins (e.g. Bell and Jefferson 1987; Dalziel 1991; Eisbacher 1985). Both the west coast of Laurentia
207 and the east coast of Australia are characterised by thick, broadly correlatable, sedimentary successions (e.g.
208 Rainbird et al. 1996; Young et al. 1979; Young 1981) that are cut by dyke swarms (e.g. Ernst et al. 2008).
209 These reconstructions placed the margin of eastern Antarctica against the southwest United States margin
210 (called SWEAT), with the east coast of Australia aligning with the Wopmay Belt of north-eastern Canada
211 (Moores et al. 1991) (Fig. 1a).

212

213 *AUSWUS*

214

215 The AUSWUS (Australia-Western United States, Fig. 1b) connection was originally proposed based on the
216 structural relationship of the offsets from three transform faults between Laurentia and Australia, and then
217 using them to more accurately align the margins (Brookfield 1993). Karlstrom et al. (1999; 2001) refined this
218 connection (terming it 'AUSWUS') by connecting the Grenvillian orogeny in Laurentia with the Albany-
219 Fraser and Musgrave orogenies in Australia and Burrett and Berry (2000; 2002) expanded on it further,

220 matching the Broken Hill and Mt Isa Terranes in Australia with the Mojavia province and San Gabriel terrane
221 in the western United States, suggesting a stronger affinity between eastern Australia and Western US, than
222 Australia and Canada.

223

224 *AUSMEX*

225

226 AUSMEX (Australia-Mexico) was proposed by Wingate et al. (2002) in response to perceived poor reliability
227 in paleomagnetic data during the latest Mesoproterozoic that made both SWEAT and AUSWUS models
228 untenable (though this was later resolved by Schmidt et al., 2006). They proposed that if Australia–East-
229 Antarctica was connected to Laurentia at all in the late Mesoproterozoic, then it could only be a marginal
230 connection with northern Queensland with Mexico. This reconstruction was done using a new paleomagnetic
231 pole from WA to constrain Australia’s location at 1050 Ma (Fig. 1c). A paleomagnetic pole from the Officer
232 Basin at 780 Ma provides a stronger argument for an AUSMEX-type configuration than either SWEAT or
233 AUSWUS when compared to similar-aged Laurentian poles (Pisarevsky et al. 2007) though it doesn’t
234 completely disqualify the other configurations. A notable problem with the AUSMEX configuration is the
235 absence of geological evidence that supports this configuration. Greene (2010) argued for an AUSMEX
236 configuration (or Missing Link configuration) based on the mismatch strike of rifting basins within Australia
237 and Laurentia.

238

239 *Missing-Link*

240

241 The Missing-Link model was originally proposed by Li et al. (1995) with the South China Cratons acting as a
242 continental slither caught between the amalgamation of Australia–East-Antarctica and Laurentia in an
243 otherwise typical SWEAT configuration (Fig. 1d). While the broad stratigraphy across eastern Australia-
244 Laurentia is congruent, there are a number of mismatches such as geochemical discontinuities (Borg and
245 DePaolo 1994) and the mantle plume record during the Neoproterozoic. Other issues exist such as
246 mismatched stratigraphy (Li et al. 2008), but are either difficult to disprove or prove concisely due to ice cover

247 in Antarctica, or they disallow a SWEAT connection for a late Mesoproterozoic but not necessarily the
248 Neoproterozoic.

249

250 The Missing-Link model neatly accounts for these, as South China shares a similar stratigraphy with both
251 Australia and Laurentia and has been used to explain the magmatic dyke record across all three cratons (Li et
252 al. 1999). The offset provided by positioning this block between Australia and Laurentia also alleviated some
253 of the problems fitting the timing of rifting within paleomagnetic constraints of Australia, though the 40°
254 intraplate rotation suggested by Li and Evans (2011) offered a neat solution re-validating SWEAT-like
255 configurations. A controversial component of the Missing-Link model is the presence of extensive magmatism
256 in South China in the early Neoproterozoic (e.g. Du et al. 2014; Zhao et al. 2011). Li et al. (1999; 2008)
257 ascribed these to rifting and intra-continental intrusions, though recent geochemistry suggests that they are
258 from active subduction zones, suggesting that South China needs to face an open ocean and not occupy a
259 central position of Rodinia (Du et al. 2014).

260

261 **Paleomagnetic constraints of Rodinia Breakup**

262

263 *Australian Constraints*

264

265 Paleomagnetic data from the Albany-Fraser Orogeny and the Gnowangerup–Fraser Dyke Suite during the
266 Late Mesoproterozoic (~1.2 Ga) requires Australia to be situated at polar latitudes (Pisarevsky et al. 2003;
267 2014), while comparable data from Laurentia places it closer to the equator (Palmer et al. 1977). From 1070
268 Ma paleomagnetic data permit a connection between Australia and Laurentia (e.g. Schmidt et al. 2006;
269 Wingate et al. 2002) in an AUSMEX type fit; with SWEAT, AUSWUS and Missing-Link type fits being
270 permissible from 1050 Ma (Powell et al. 1993). There is little reliable Australian paleomagnetic data from the
271 early Neoproterozoic (Table 1), which makes it difficult to discriminate between both the differing
272 configurations and rifting time, though poorly dated results from the 830-720 Ma Buldya Group, constrain its
273 position to low-latitudes (Pisarevsky et al. 2007) (Fig. 2-4). In particular, an 825 Ma pole from the Browne
274 Formation (though there are uncertainties on the age of the sediments in the Browne Formation (cf. Schmidt

275 2014)) and a 780 Ma pole from the Hussar Formation suggests low latitudes, with the latter pole favouring an
276 AUSMEX configuration *if* Australia-Laurentia had not separated yet (Fig. 2a, b) (Pisarevsky et al. 2007).

277

278 Two paleomagnetic 'grand-poles' (mean of two or more key-poles from separate laboratories) from
279 Precambrian Australia were determined for the late Neoproterozoic by Schmidt (2014) in his recent review.
280 The first, from the Mundine Dyke Swarms (MDS), combines a 755 Ma pole (Wingate and Giddings, 2000)
281 with a 748 Ma pole (Embleton and Schmidt, 1985), and the second encompasses the Elatina Formation (EF),
282 and is dated at ~635 Ma (Schmidt et al. 2009; Schmidt and Williams, 1995; Sohl et al. 1999). The former pole
283 places Australia at low latitudes and was interpreted to constrain rifting to ~750 Ma at the latest (Wingate and
284 Giddings, 2000) (Fig. 3b); however the 40° intraplate rotation of Li and Evans (2011) permits rifting to
285 continue later (until ~700 Ma), by reconciling the MDS with the ~770-750 Ma Walsh Tillite Cap pole
286 (Li 2000). A ~770 Ma pole from the Bitter Springs in central Australia by Swanson-Hysell et al. (2012) also
287 supports this intraplate rotation, as the rotation reconciles this pole with the MDS pole (Schmidt 2014) (Fig.
288 3a).

289

290 Paleomagnetic data are available for the Ediacaran in Australia, with a series of poles from 650-580 Ma,
291 including the EF grand pole (Schmidt et al. 2009; 2014) that constrain its position from equatorial to sub-
292 equatorial (Schmidt et al. 2009, Schmidt and Williams 1996; 2010; Sohl et al. 1999), but having rotated
293 counterclockwise relative to Laurentia, such that it is aligned NW-SE as opposed to NE/E-SW/W (depending
294 on starting configuration) within Rodinia (Fig. 4a,b). The Yaltipena formation (Sohl et al. 1999) (Fig. 4a),
295 taken here as ~650 Ma after Li et al. (2013), and on the basis that it must be older than the Elatina glaciation
296 which has a maximum age of 640 Ma (Schmidt 2014; Williams et al. 2008) (Fig. 4b) is the start of the
297 Australian Ediacaran polar wander path, which indicates that Australia drifted in low latitudes (Schmidt and
298 Williams 2010). At some time in the Neoproterozoic prior to 650 Ma, Australia (together with East-
299 Antarctica) must rift from Laurentia to reach this position, and we use this position as our common end point
300 for all configurations.

301

302 We note that SWEAT, AUSWUS and AUSMEX are all problematic with younger rifting times (younger than
 303 ~770 Ma) on paleomagnetic grounds due to the mismatch between the MDS pole and equatorial position of
 304 Laurentia, which, given these fits, would have to sit N-S (similar to present day) rather than E-W (Wingate
 305 and Giddings 2000). Importantly, the position of Australia in the Missing-Link Model helps minimise the
 306 offset of the MDS pole (as it is situated more 'upright' relative to Laurentia).
 307

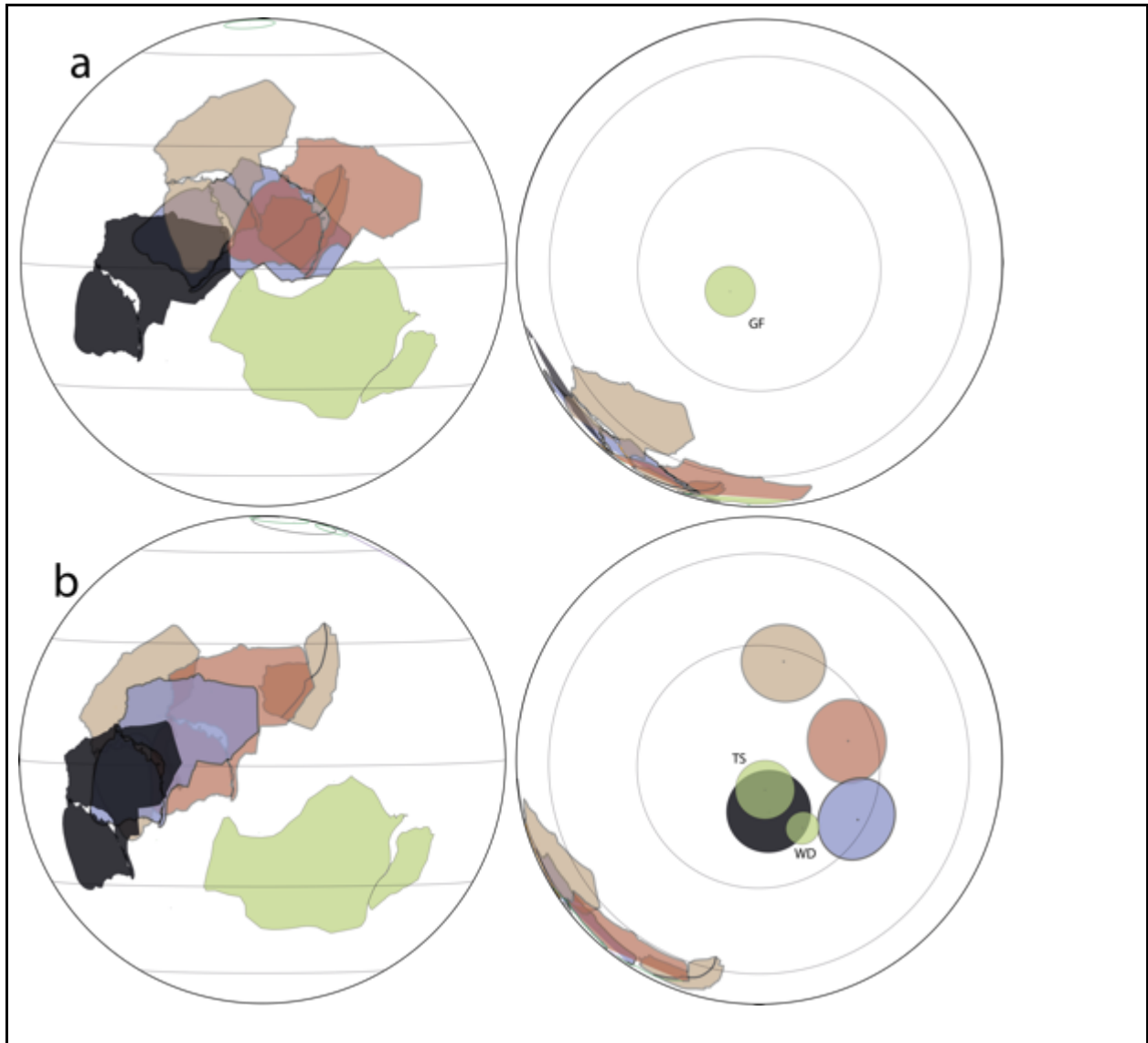


Figure 2: Paleomagnetic data for Australia and Laurentia at (a) 800 Ma, and (b) 780 Ma. Alternate Australia configurations are colour-coded; SWEAT, red; AUSWUS, blue; AUSMEX, black; Missing-Link, tan. Laurentia is in green. GF, Galeros Formation, TS, Tsezotene Sills, WD, Wyoming Dykes. Australian

pole in (b) is the Hussar Formation.

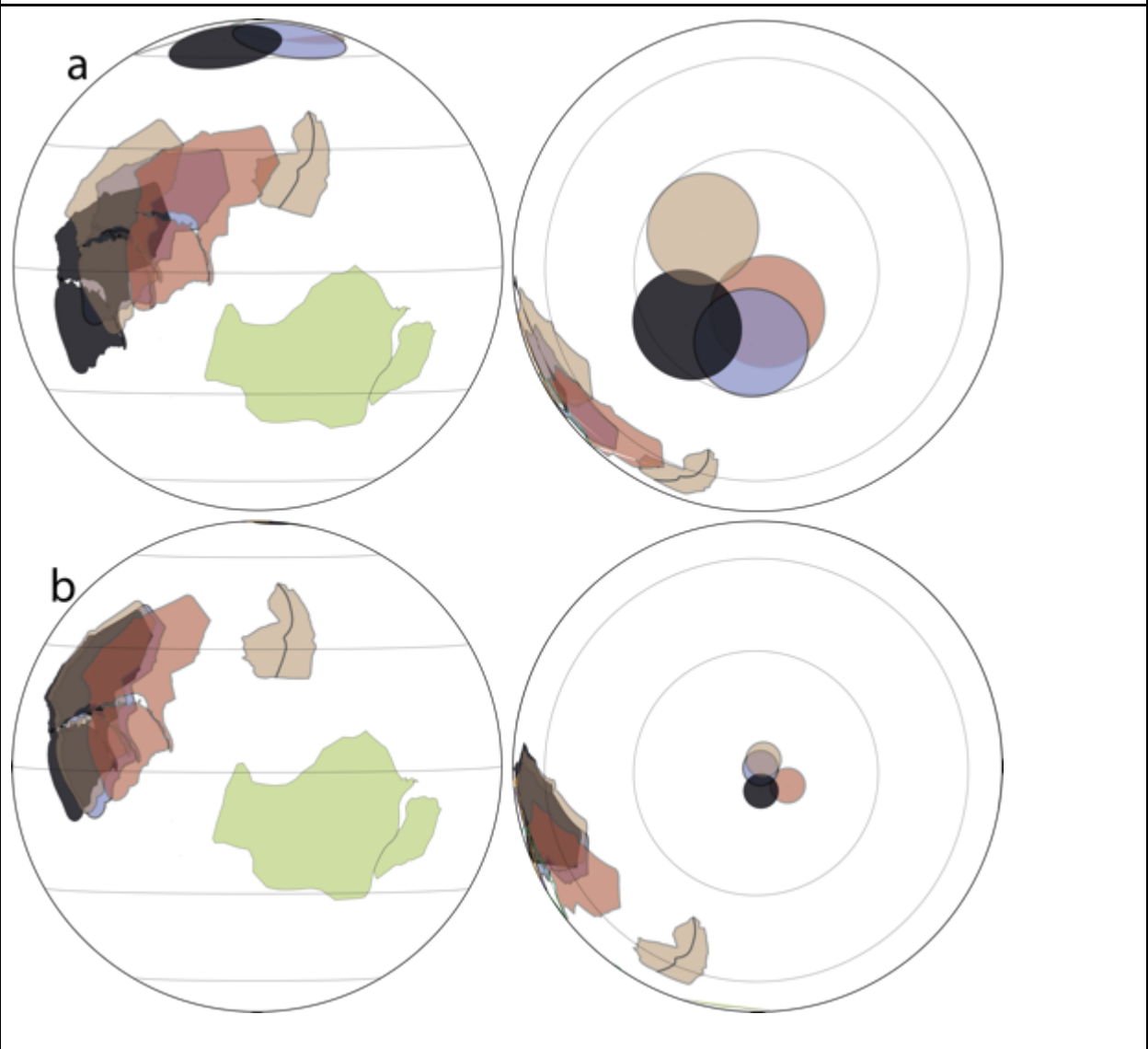


Figure 3. Paleomagnetic data for Australia and Laurentia at (a) 770 Ma (Johnny Creek Pole), and (b) 750 Ma ('grand-pole' from Mundine Dyke Swarms). Alternate Australia configurations are colour-coded; red, SWEAT; blue, AUSWUS; black, AUSMEX; orange, Missing-Link. Laurentia is in green.

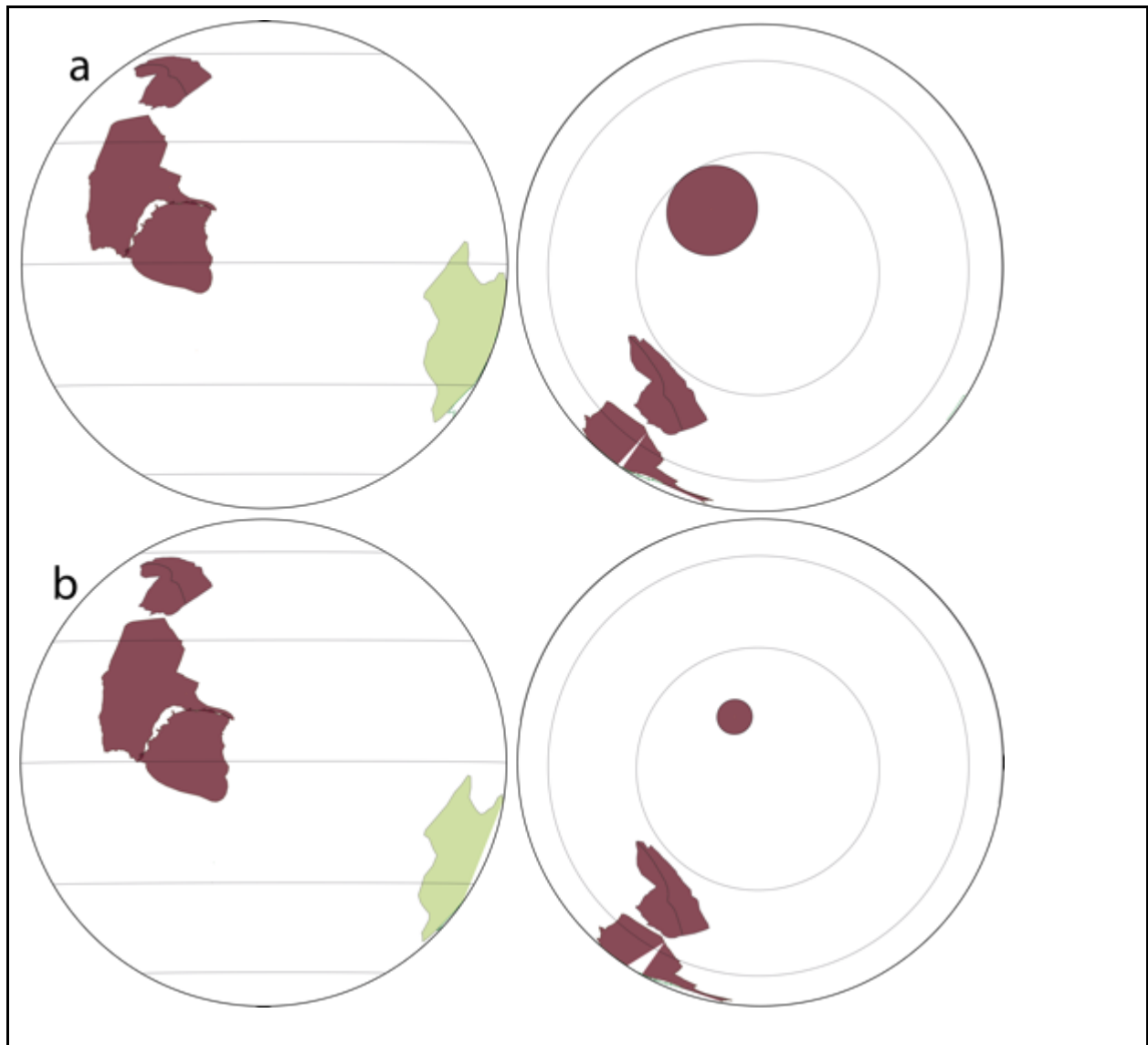


Figure 4. Paleomagnetic data for Australia and Laurentia at (a) 650 Ma, and (b) 640Ma. The alternate Rodinian configurations for Australia are now synonymous (red) and Laurentia is in green. Australian poles are Yaltipena Formation (a) and the 'grand-pole' of the Elatina Formation (b).

308

309

310 *Laurentia*

311

312 Only a few poles constrain Laurentia's position between 830-650 Ma. Two higher quality poles, the 782 Ma

313 Wyoming Dykes (Harlan et al. 1997) and the 779 Ma Tsezotene sills and dykes (Park et al. 1989), both

314 indicate Laurentia lying at low latitudes (Fig. 2b). A ca. 720 Ma pole from the Natkusiak volcanics in the
315 Franklin magmatic event limits Laurentia to a low latitude (Denyszyn et al. 2009). Finally, two poorly-dated
316 poles from the Galeros and Kwagunt Formations (800-740 Ma) (Fig. 2a) also suggest a low latitude Laurentia
317 during this time (Weil et al. 2004), though the lack of a reliable age makes them difficult to use in
318 reconstructions. No paleomagnetic data exists for Laurentia (or Baltica and Amazonia) at ~650 Ma with the
319 closest reliable pole on the younger side from the Long Range Dykes (Murthy et al. 1992) placing Laurentia
320 equatorially at 615 Ma. We follow Li et al. (2008; 2013) in assuming a simple interpolation between the two
321 poles, leaving Laurentia at equatorial latitudes during this time.

322

323 **Assembly of Eastern Gondwana**

324

325 *Paleomagnetic Data*

326

327 Paleomagnetic data from India are incredibly sparse, hence the uncertainty attached to its position by nearly
328 all global tectonic models of the Neoproterozoic (Table 1). Positions include having it attached to
329 northwestern Australia (e.g. Li et al. 2008) attached to western Australia–East-Antarctica (similar to its
330 Gondwana position) (e.g. Dalziel 1991; Hoffman 1991; Moores 1991), or not part of Rodinia at all (Powell
331 and Pisarevskyb 2002; Torsvik et al. 2001a;b). Generally, it's relative position is always to the north-
332 west/west of Australia, such that by ~650 Ma subduction of the ocean separating it from Australia leads
333 towards Gondwana amalgamation. A ~770 Ma pole from the Malani Igneous Suite (Gregory et al. 2009,
334 Torsik et a, 2001b) indicates a mid-latitude position for Neoproterozoic India at this time (Fig. 5a), and is
335 supported by a ~750 Ma pole from the Seychelles that indicates a similar position (Torsvik et al. 2001a).
336 Chronologically, the next Indian pole is that from the Bhandar and Rewa Series at ~550 Ma, which constrains
337 it to a sub-equatorial position, and is coeval with the final collision of India-Congo (Fig. 5b) (McElhinny et al.
338 1978). India's motion between these two poles is generally interpreted to be drifting south, which suggests that
339 it wasn't part of a Rodinia through this time.

340

341

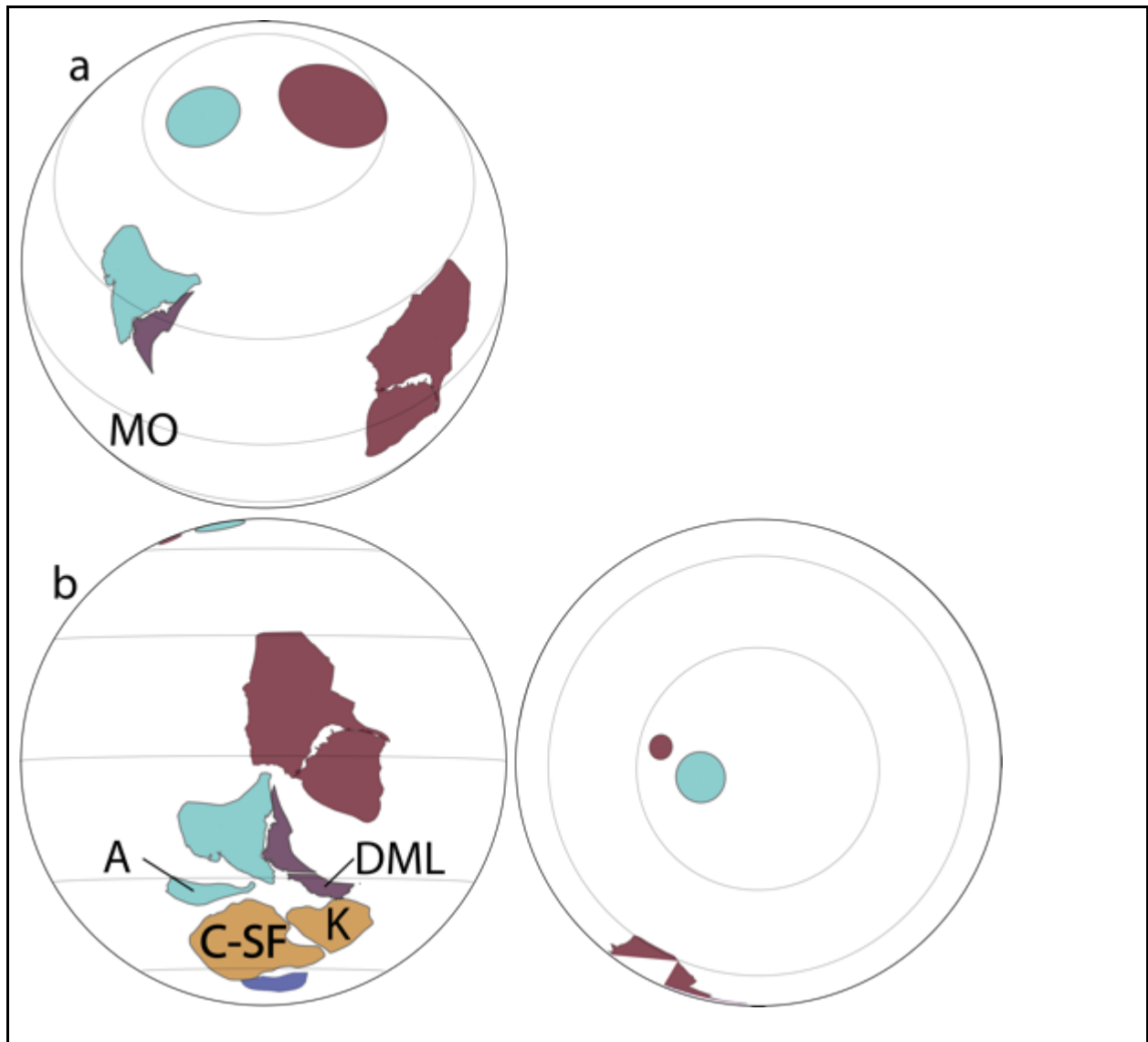


Figure 5. Paleomagnetic data for India at (a) 770 Ma (Malani Igneous Suite), and (b) 550 Ma (Bhander and Rewa Series). India in light blue; A, Azania; C-SF, Congo-Sao Francisco Craton; K, Kalahari craton; MO, Mozambique Ocean; Australia and Antarctica in purple,. Australian poles are the (a) Johnny Creek pole and (b) the 545 Ma Upper Arumbera Sandstone (Kirschvink 1978).

342

343

344 *Geological Data*

345

346 The assembly of eastern Gondwana was driven primarily by the subduction of the Mozambique Ocean
347 forming two major orogenies, the East African Orogen (divided by Collins and Pisarevsky 2005 into the East
348 African orogeny that was the collision of the Arabian Nubian Shield/Azania with Congo/Sahara, and the
349 Malagasy orogeny, the collision of continental India with Congo based on distinct collisional ages) between
350 India and Congo, and the Kuungan (or Pinjarra in Australia) Orogeny between India and Australia–East-
351 Antarctica (Meert 2003). Detailed geological synopsis of this collision have been undertaken previously (e.g.
352 Boger et al. 2015; Collins et al. 2014; Johnson et al. 2005), and we summarise below the pertinent geological
353 observations available to constrain relative plate motion between India-Australia and India-Gondwana that
354 links absolute positions constrained by paleomagnetic data.

355
356 Southward movement of India during the Cryogenian suggested by paleomagnetic data is broadly compatible
357 with the geological record, where preserved ophiolites in the Manumedu Complex suggest not only supra-
358 subduction zone roll-back between 800-700 Ma, but also that this formed the southern extent of
359 Neoproterozoic Greater India (e.g. Collins et al. 2014; Yellappa et al. 2010). Southern India consists of a core
360 of cratonised Archean-aged crust, the Dharwar Craton, and the Southern Granulite terrane, a series of
361 Neoproterozoic and Proterozoic-aged terranes broadly younging southwards through; the Northern Madurai
362 Block and Southern Madurai Block, which are separated from the Palaeoproterozoic Trivandrum Block and
363 Nagercoil Blocks by the Achankovil Shear Zone (Collins et al. 2014). Collins et al. (2014) and Plavsa et al.
364 (2014) show that these southern blocks of present-day India were likely to be part of Azania and the Malagasy
365 arc (Archibald et al. 2015), outboard of the Congo craton, on the basis of detrital zircon signatures and
366 similarities in metaigneous rocks, so that by the mid-Neoproterozoic a backarc basin (termed Neomozambique
367 Ocean by Plavsa et al. 2014) separated Congo from Azania (and southern Indian blocks), and the larger
368 Mozambique ocean separated Azania from India. Greater India entered a period of tectonic quiescence from
369 ~700-625 Ma, though on the other side of the Mozambique ocean, Azania records convergence-related
370 deformation and metamorphism from ~675-500 Ma (Ashwal et al. 1998; Buchwaldt et al. 2003; Collins 2006;
371 Collins et al. 2014; Wit et al. 2001). The Malagasy orogeny is recorded in Azania (and the southern India
372 blocks) from ~625-500 Ma (Collins et al. 2014), with an inferred collision between it and Greater India at
373 ~550 Ma (e.g. Boger 2011; Collins and Pisarevsky 2005; Meert 2003).

374

375 The synthesis of paleomagnetic and geological data suggests a continuous southerly drift of India during the
376 Cryogenian, with a subduction reversal, at ca. 700 Ma onto the southern margin of the Mozambique Ocean
377 (i.e. north side of Azania), resulting in destruction of this ocean basin. Synchronously, subduction of the
378 Neomozambique Ocean under Congo occurred, resulting in the closure of the basin between Congo-Azania.
379 This created double-dipping subduction (Plavsa et al. 2014) and resulted in a perpendicular, 'head on' collision
380 between India and Gondwana (Collins et al. 2014), the evidence for which, in part, is shown by the granulite
381 facies metamorphism recorded in the Mozambique suture (e.g. Collins et al. 2007; Fitzsimons 2016).

382

383 The motion of India relative to Australia during the mid-late Neoproterozoic (i.e. ~750-550 Ma) was originally
384 envisioned as relatively minor and intra-continental (Harris and Beeson 1993). This was largely due to an
385 interpretation of the metamorphism and magmatism in the intervening region as being due to crustal thinning
386 and strike-slip deformation rather than crustal thickening and plate convergence. This interpretation was
387 revised during the 2000's with studies of the metamorphism, deformation and geochronology of SW Australia
388 (Collins, 2003), the Prydz Bay area of Antarctica (Kelsey et al. 2007) and NE India (Yin et al. 2010) that
389 concluded that the Neoproterozoic orogen between India and Australia in Gondwana represented periodic
390 ocean subduction and crustal thickening – a true oceanic suture. To explain the (now necessary) relative
391 motion of India to Australia during Gondwana assembly times, a sinistral strike-slip motion along the Darling
392 Fault in Western Australia is used (e.g. Collins 2003; Fitzsimons 2003; Harris 1994; Powell and Pisarevsky
393 2002), suggesting that India was dragged south, past Australia, into a collision with Gondwana.

394

Location	Age (Ma)	Pole		A95	Reference
		°N	°E		
Australia					
Browne Formation	830-800 Ma	44.5	141.7	7.9	Pisarevsky et al. 2007
Hussar Formation	800-760 Ma	62	86	14.6	Pisarevsky et al. 2007
*Johnny's Creek	780-760	15.8	83	13.5	Swanson-Hysell et al. 2012
*Mundine Dyke Swarms ('Grand Pole')	750	45.3	135.4	5	Embleton and Schmidt, 1985; Schmidt 2014; Wingate and Giddings, 2002
*Yaltipena Formation	650	-44.2	352.7	11	Sohl et al. 1999
*Elatina Formation ("Grand Pole")	635	-43.7	359.3	4.2	Schmidt 2014; Schmidt and Williams, 2010
Laurentia					
Galeros Formation,	800-780	-2	163	6	Weil et al. 2004
*Wyoming Dykes	785±8	13	131	4	Harlan et al. 1997
*Tsezotene Sills,	779±2	2	138	5	Park et al. 1989
Kwagunt Fomration	742±6	18	166	8.4	Weil et al. 2004
Franklin-Natkusiak Magmatic Event	720	8	164	2.8	Denyszyn et al. 2009
India					
*Malani Igneous Suite	770	68	73	9	Gregory et al. 2009
*Bhander and Rewa Series	550	47	213	6	McElhinny et al. 1978

397 **Formulation of Analysis**

398

399 For Australia—East-Antarctica and Laurentia rifting, we generated alternative scenarios as follows:

400

- 401 • Alternative starting configurations were based on published poles of rotation (Fig. 1)
- 402 • The Euler Pole describing Australia’s position at 650 Ma is the same for all configurations, and defined by
403 the beginning of the magnetostratigraphy of the South Australian sedimentary sequences (e.g. the
404 Yaltipena, Elantina, Nuccaleena, Bunyeroo Formations)
- 405 • Variations of rifting time between Australia–East-Antarctica and Laurentia were generated in 25 Myr
406 time steps from 800-725 Ma to examine how spreading rates change, with earlier rifting times adjusted by
407 the insertion of a new Euler pole rotation at 750 Ma in order to satisfy the latitudinal position of the MDS
408 pole

409

410 Though SWEAT, AUSWUS, AUSMEX configurations are paleomagnetically problematic with later rifting
411 times (post ~770 Ma), we include their analyses to further highlight whether late rifting is likely or not.
412 Consequently, this creates a 30° mismatch the MDS pole and the reconstructions for rifting at 750 and 725 Ma
413 for these configurations. Additionally, we do not include the intraplate rotation of the North Australian
414 Craton to the South Australian Craton of Li and Evans (2011) because both AUSMEX and AUSWUS were
415 proposed before this rotation was introduced, and neither model has been tweaked to incorporate it.

416

417 Absolute constraints on paleolongitude have been explored for the Paleozoic (e.g. Torsvik et al. 2008), though
418 there is yet to be a method for constraining longitude in the Precambrian. As we are looking at relative plate
419 motions between times of absolute plate position (i.e. constrained by paleomagnetic data) the relative
420 longitudinal constraints are bound by satisfaction of three criteria:

421

- 422 • Latitudinal positions as described by paleomagnetic data (i.e. we assume simple, continuous paths
423 between the paleomagnetic end points)

424 • Geological data, specifically regarding major blocks colliding, sharing a connection, or separating
425 from one another

426 • Kinematic criteria evidenced from present day ocean basins - reconstructions should be considered
427 more likely where the spreading rates within oceans forming after continental rifting are reasonable

428
429 To deal with uncertainties in paleolongitude we calculate a range of possible widths for the Paleopacific Ocean
430 (between Australia—East-Antarctica, Kalahari and Laurentia) at 650 Ma based on slow (20 mm/yr) and fast
431 (120 mm/yr) spreading, while constraining the latitudinal position of each continent to remain consistent with
432 paleomagnetic data.

433
434 For the Gondwana amalgamation we reconstructed India-Australia and India-Congo motions we used the
435 following criteria:

- 436
- 437 • Start position of Australia—East Antarctica is from 650 Ma and follows the Australian Ediacaran
 - 438 APWP (Schmidt and Williams 2013, Schmidt et al. 2014)
 - 439 • Congo at 550 Ma is situated mid-latitudes using a mean Gondwana pole (Torsvik et al. 2012)
 - 440 • India is interpreted to have a southward motion based on the closure of the Neomozambique and
 - 441 Mozambique ocean under Congo and Azania respectively
 - 442 • India collided head on with Congo
 - 443 • A sinistral transform fault separated Australia—East Antarctica from India between 650-550 Ma this
 - 444 time

445
446 To assess the relative plate motions implied by Neoproterozoic plate models, we consider the post-Pangea
447 evolution of the ocean basins. Figure 6a shows the fracture zones of the present day ocean basins (Matthews
448 et al. 2011; Wessel et al. 2015) and indicates that rapid changes in the orientation and rate of seafloor
449 spreading can occur *when* they coincide with changes in the global plate regime. For example, the change in
450 the Indian Ocean is due to the onset of rifting between Australia and Antarctica at 40 Ma. Figure 6b shows
451 the most recent compilation of seafloor spreading rates since Pangea breakup (Müller et al. 2016). The global

452 mean spreading rates of currently preserved ocean crust is 37 mm/yr, with a standard deviation of 27 mm/yr
453 (Fig. 6b). We take the optimal range of spreading rate to be 10-70 mm/yr, though we note that faster rates of
454 spreading can be acceptable in certain circumstances, such as plates without cratonic lithospheric roots or
455 plates comprised predominantly of oceanic crust (Zahirovic et al. 2015). We also note that as continental-
456 continental collision occurs, the convergence rate of the moving plate slows, as suggested by India's collision
457 with Eurasia (Cande and Patriat, 2015; van Hinsbergen et al. 2011). Finally, based on Bird (2003) and Argus
458 et al. (2010; 2011) the angular rotation for cratonic landmasses in the present day is $< 5^\circ/\text{Myr}$ though smaller
459 plates without cratonic crust can exhibit faster (up to $20^\circ/\text{Myr}$) rates of angular rotation.

460

461 Six sets of kinematic data were extracted; flowlines, position and angular rotation of Euler poles that describe
462 the motion, relative spreading rates, and, mid-ocean ridge orientation, were extracted from the relative
463 motions of Australia-Laurentia rifting and Kalahari-Laurentia rifting, and motion paths and convergence rates
464 were extracted from the relative motion of India to Congo and Australia. Kinematic data were analysed at a
465 regular time interval of 5 Myr, although, provided a full reconstruction is supplied, this can be altered to be of
466 any temporal resolution. For the assembly of Gondwana, motion paths and convergence rates were extracted
467 from the relative motion of India-Australia and India-Congo. The rotations of other continental plates, while
468 not used for the analysis, were plotted to help with visual reference by placing Australia, India, Congo and
469 Laurentia within a global context. The rotations of these continents were adapted from Li et al. (2008; 2013).

470

471

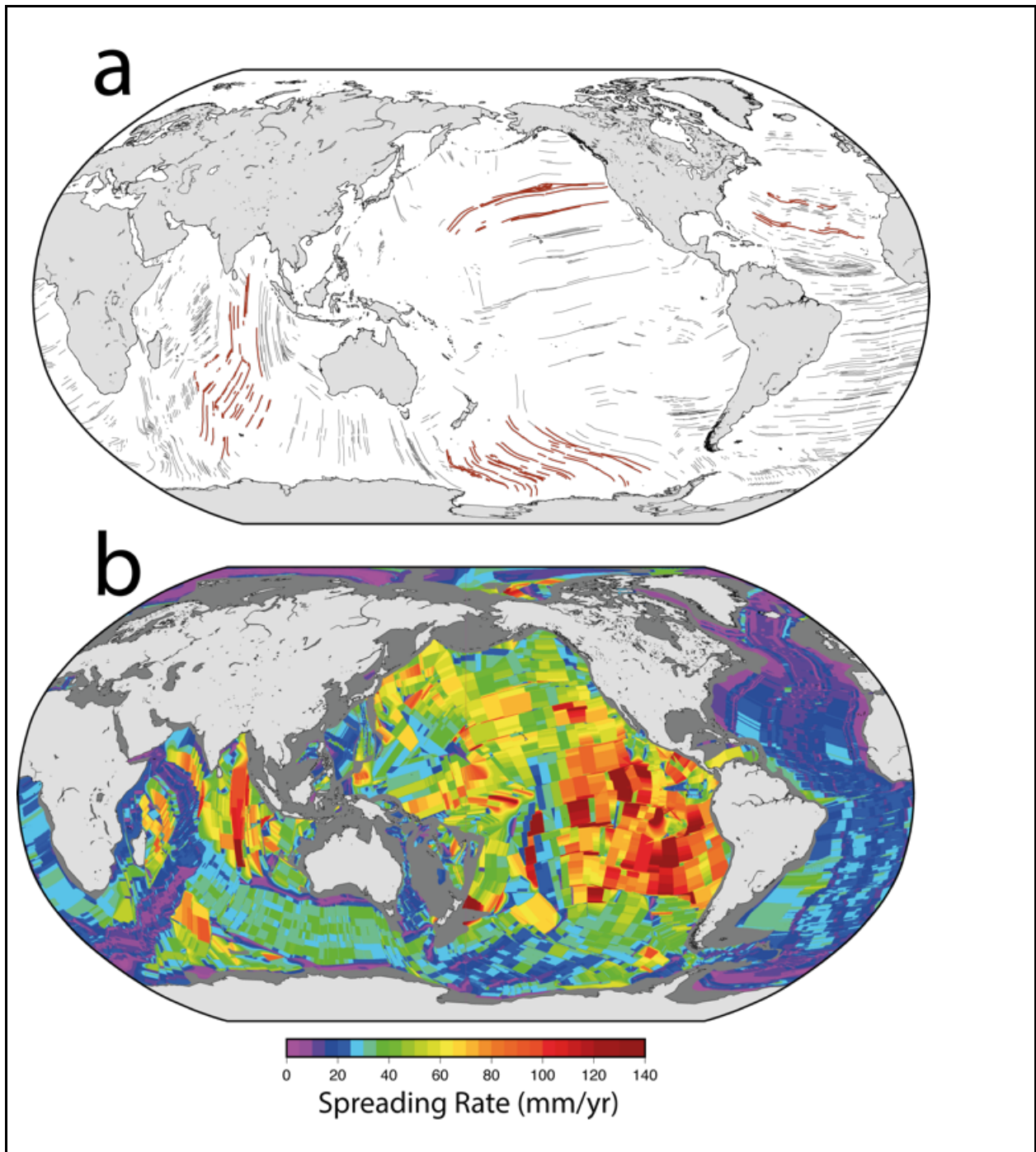


Figure 6: (a) Seafloor fabric map of the world after Matthews et al. (2011) showing the nature of present day fracture zones and spreading. In particular we highlight the rapid changes of spreading direction that occur regularly in the modern day ocean basins (visible along fracture zones highlighted red). (b) Seafloor spreading rate of the world's ocean basins based on Müller et al. (2016). The mean global spreading rate in

ocean floor preserved today is ~ 37 mm/yr, with a standard deviation of 27 mm/yr.

472

473

474 **Results**

475

476 Results are presented below in Figures 7, 8 and Table 1. SWEAT, AUSWUS and AUSMEX all have
477 comparably simple rifting patterns and flowlines, while the Missing-Link model has a more convoluted
478 spreading history. The present day range of spreading rates is plotted in black for each configuration for
479 comparison. Average rates of motion refer to the average across all synthetic flowlines, while the maximum
480 rate of motion refers to the single instance of maximum motion on any flowline for the specific configuration
481 and rifting time.

482

483 **Rodinia breakup**

484

485 In SWEAT configurations the flowlines are simple, and the degrees of angular rotation are low for an 800 Ma
486 rifting time, (~ 1 °/Myr) but higher for 750 Ma and 725 Ma rifting times (1.3 °/Myr and 1.7 °/Myr
487 respectively), and divergence rates increase with later rifting times (average/maximum 76/94 mm/yr at 800
488 Ma and 149/170 mm/year at 725 Ma). Divergence direction changes from 210° at rifting time towards 290°
489 at 650 Ma (Fig. 7a).

490

491 AUSWUS configurations show simple flowlines with the degrees of angular rotation increasing as the timing
492 of rifting gets younger (from 1.5 °/Myr at 800 Ma to 1.8 °/Myr at 725 Ma) (Fig. 7b). The relative spreading of
493 the plates away from each other is much lower with earlier rifting (average/maximum rates 56/73 mm/year
494 for 800 Ma) and increases as rifting time decreases (average/maximum, 120/147 mm/year for 725 Ma) (Fig.
495 7b). For all rifting times the orientation of spreading changes from 220°, at rifting time, to 290° at 650 Ma
496 (Fig. 7b).

497

498 The kinematics for AUSMEX configurations have similar results to AUSWUS configurations. Angular
499 rotation is highest at 725 Ma where it reaches $1.6^{\circ}/\text{Myr}$. The divergence rates follow the same pattern as
500 AUSWUS, increasing as rifting time decreases (average/maximum, 64/87 mm/yr with rifting at 800 Ma and
501 113/135 mm/yr at 725 Ma rifting, Fig. 7c) and rifting orientation increases stepwise from 220° at rifting time
502 to 300° at 650 Ma (Fig. 7c).

503

504 The Missing Link configurations have the most complex flowlines of all configurations, depicting a series of
505 reorganisations between rifting time and 650 Ma (Fig. 7d). All rifting times have periods of angular rotation at
506 $\sim 2^{\circ}/\text{Myr}$, and the orientation of seafloor spreading changes more regularly than other configurations, with
507 five different adjustments occurring between rifting time and 650 Ma for 800 and 775 Ma, four for 750 Ma,
508 and three for 725 Ma. Average spreading rates mimic that of the other configurations, being slowest at earlier
509 rifting times (90 mm/yr at 800 Ma) and higher at younger rifting times (150 mm/yr at 725 Ma), though all
510 rifting times have similar maximum spreading rates of ~ 210 mm (Fig. 7d). In all cases the orientation of the
511 spreading ridge varies between 60° and $270^{\circ}/\text{Myr}$ (Fig. 7d).

512

513

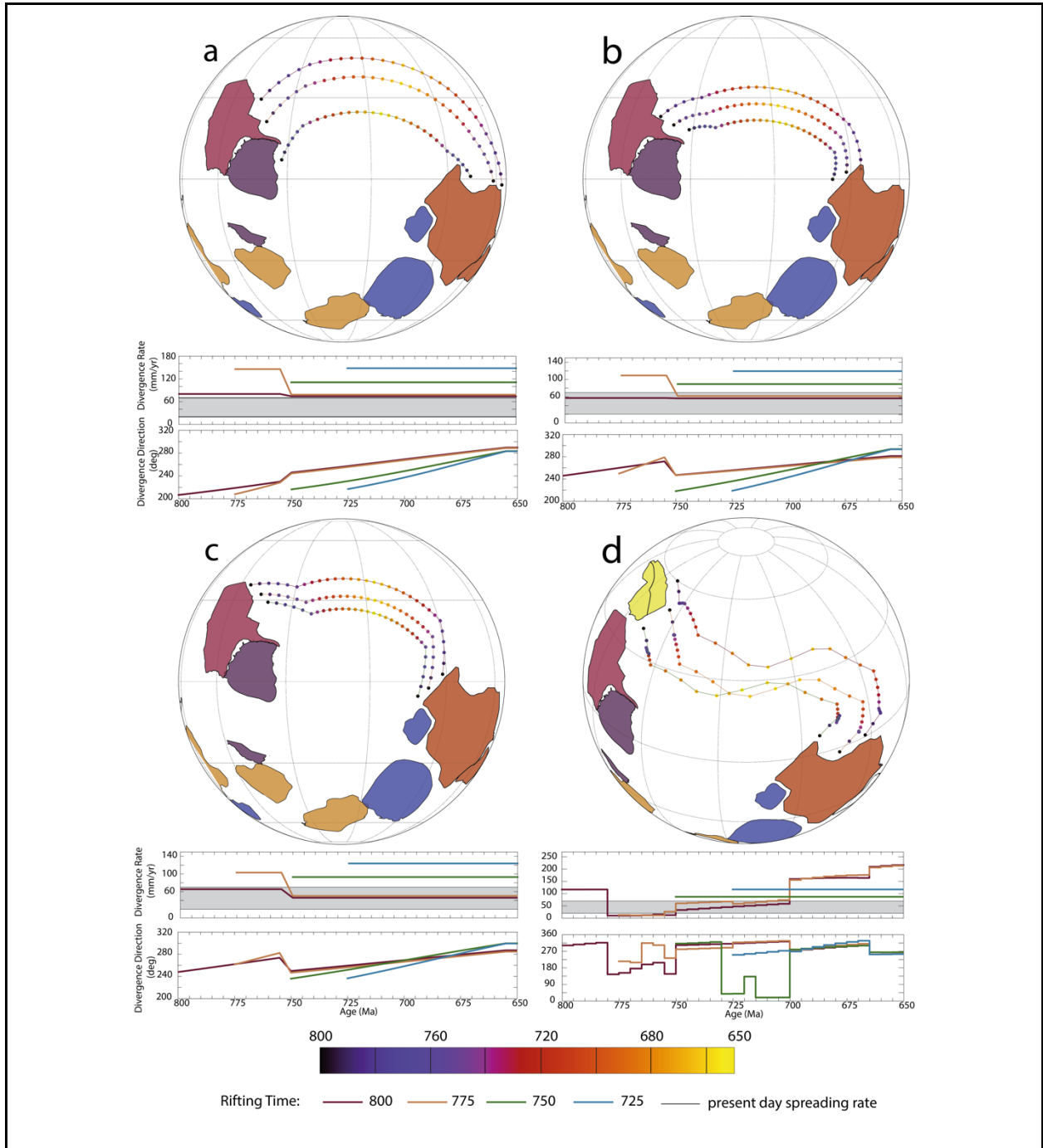


Figure 7: Kinematic results from Neoproterozoic Australia-Laurentia configurations, (a) SWEAT, (b) AUSWUS, (c) AUSMEX, (d) Missing-Link. Flowlines depicted are of rifting at 800 Ma, results for spreading rates and orientation of spreading are colour coded by rifting ages. South American cratons are dark blue; Africa, orange; India, light blue; Antarctica, purple; Australia, scarlet; Laurentia, red; and, South China, yellow.

514
515
516
517
518
519
520
521
522
523
524
525
526
527
528
529
530
531
532
533

Longitudinal separation of Australia and Laurentia at 650 Ma

The two criteria governing Laurentia's (and West Africa and Amazonia that were attached to Laurentia) paleolongitudinal position are ensuring a reasonable rate of divergence from Australia, and ensuring that it drifts far enough to avoid early (i.e. before ~580 Ma) collision between the eastern and western Gondwanan constituents. Figure 8 shows a range of possible positions of Laurentia relative to Australia (with paleolatitudes consistent between all cases) given specific spreading rates at the different rifting times. To satisfy the paleolatitude constraints, at least ~3000 km of crust must be generated on both sides of the rift at a minimum (a total of 6000 km, Fig. 8, position of 'slow' Laurentia), this creates variations in the required minimum spreading rates depending on rifting time, with 800 Ma rifting able to satisfy this with a rate of 40 mm/yr, 775 Ma rifting at 48 mm/yr, 750 Ma rifting at 60 mm/yr and 725 Ma rifting at 80 mm/yr. Comparably, fast spreading rates, especially for the earlier rifting times (775 and 800 Ma) would place Laurentia ~15000-18000 km away respectively. Importantly, only these earlier rifting times can satisfy the constraints of modern day spreading rates, and for the later rifting times (750 and 725 Ma) the faster spreading rates (greater than 70 mm/yr) are required for moving Laurentia (with Amazonia and West Africa) far enough away to avoid collision with the Kalahari (Fig. 8c, d).

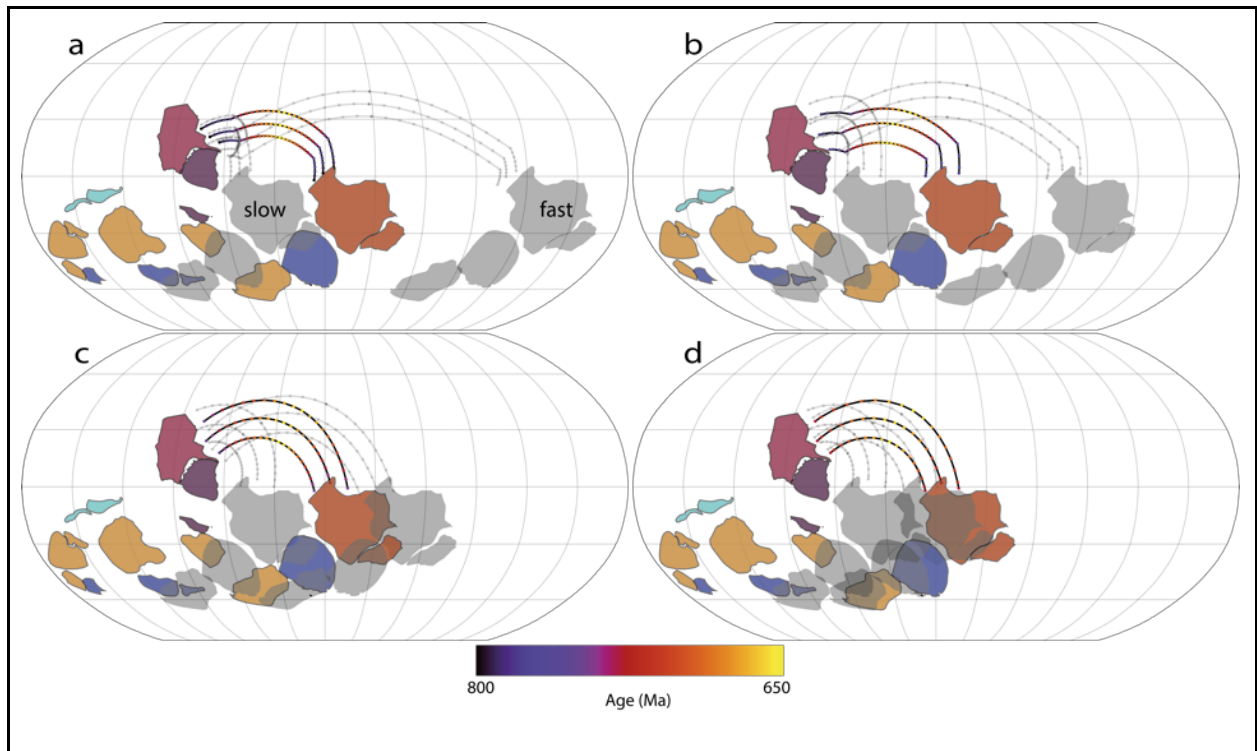


Figure 8: Laurentia and Gondwana constituents at 650 Ma with rifting at (a) 800 Ma, (b) 775 Ma, (c) 750 Ma, and (d) 725 Ma. Original configuration of Australia—East-Antarctica and Laurentia was the AUSWUS configuration, though all configurations have the same final position of Australia and Laurentia. Grey outlines are the position of Laurentia and the two major Gondwana cratons that remained attached to it, Amazonia and West Africa, but positioned if spreading rates were slow or fast (120 mm/yr). The shaded cratons are the results used in the analysis. The rate of slow spreading is determined by the minimum spreading distance between Laurentia and Australia (~6000 km) required to satisfy their paleolatitudinal position (see text).

534

535

536 **Eastern Gondwana Amalgamation**

537

538 The motion of India relative to Congo shows a front on collision of the southern tip of India with Congo,
 539 through to the north-west margin colliding with Azania and northern Madagascar. The rate of motion
 540 decreases from 60-75 mm/year between 700-650 Ma to 20-30 mm/year between 650-550 Ma (Fig. 9a).

541 Comparably, the movement of India relative to Australia (Fig. 9b) depicts a sinistral motion from 650-550 Ma
 542 between the two continents. From 550-520 Ma the motion becomes convergent as Australia–East-Antarctica
 543 collide with India forming the Kuungan orogeny. The rate of motion of India relative to Australia is 60
 544 mm/year during the transform motion, before slowing to 20-30 mm/year at 550 Ma for convergence.
 545
 546

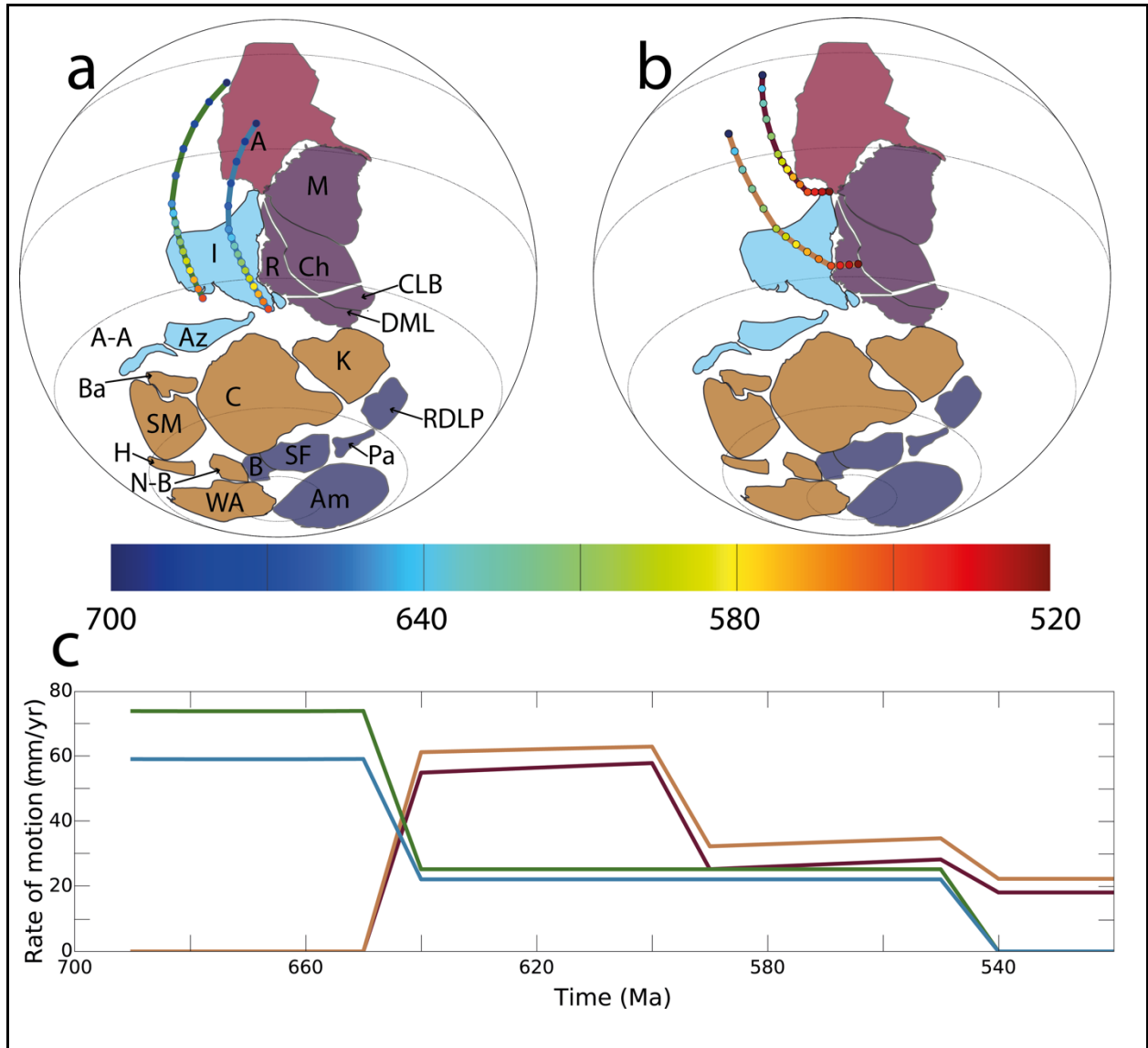


Figure 9: Kinematic results for India's motion relative to (a) Australia and (b) Congo. (c) Depicts the convergence rates of India. South American cratons are dark blue; Africa, orange; India, light blue;

Antarctica, purple; and, Australia scarlet. A, Australia; A-A, Afif-Abas; Am, Amazonia; Az, Azania; Ba, Bayuda; B, Borborema; C, Congo; Ch, Crohn Craton; CLB, Coats Land Block; DML, Dronning Maud Land; H, Hoggar; K, Kalahari; M, Mawson; N-B, Nigeria-Benin Block; Pa, Parana-Panema; R, Rayner Province; RDLP, Rio de la Plata; SF, Sao-Francisco; SM, Sahara Metacraton; WA, West Africa.

547

548

549 As India's position between 650-550 Ma is unconstrained, we determined possible positions of India relative to
550 Congo (indicated by an arc, Fig. 10) assuming motion towards the Gondwana nucleus (as suggested by
551 continuous southerly subduction) with alternative, uniform convergence rates. Slow convergence (~20
552 mm/yr) places India more southerly than Australia at 650 Ma, while convergence at 70 mm/yr places it
553 slightly further north if the strike-slip boundary with Australia is preserved. A more westerly India that follows
554 a similar convergence rate would remove this component. Fast convergence (140 mm/yr) places India
555 ~14000 km away from the Gondwana nucleus and implies a vast area of ocean being subducted.

556

557

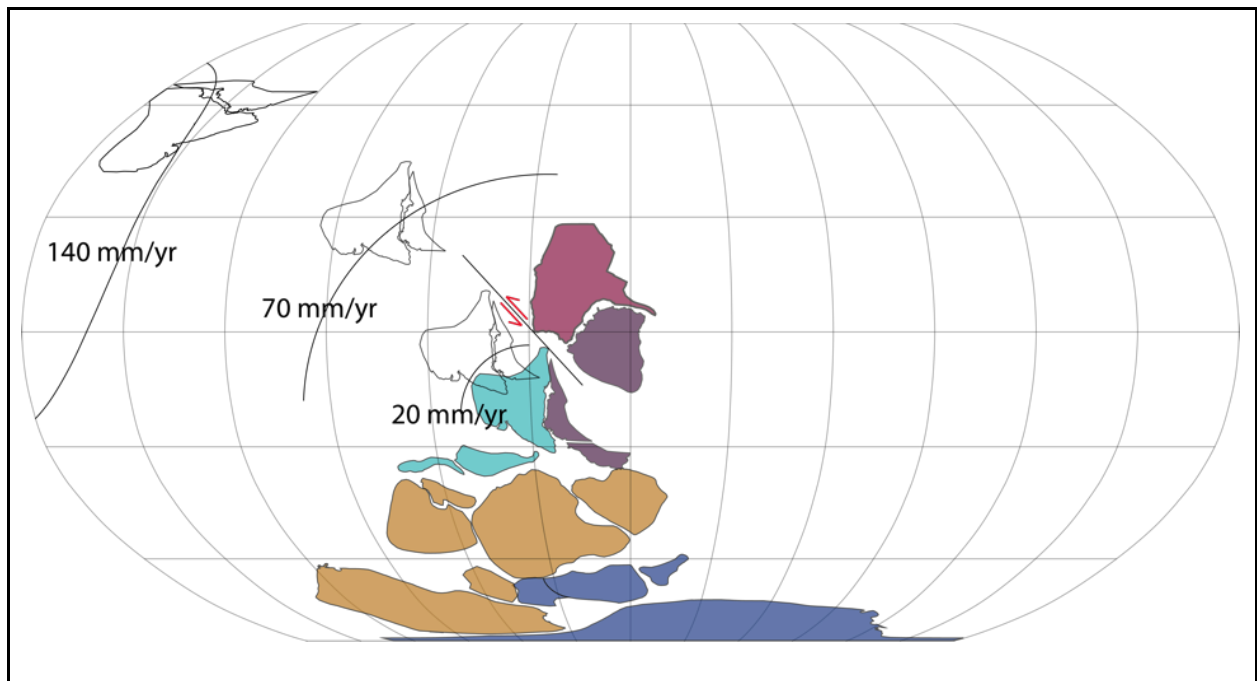


Figure 10: Possible positions of India relative to Gondwana constituents. Coloured polygons depict their

positions at 550 Ma (time of India-Congo collision). Three potential positions of India are shown based on convergence rates, they are depicted by the black arcs (i.e. India could sit anywhere along the arc and its convergence rate would be 20/70/140 mm/yr). The black shaded area is where India would be considered moving relative to Australia along a transform boundary.

558

559

560 **Discussion**

561

562 **Spreading and convergence rates**

563

564 As the final position of Australia at 650 Ma is the same for all configurations (defined latitudinally by
565 paleomagnetic data), Australia *must* move a similar distance for each rifting time. Consequently, its angular
566 rotation varies only by how the orientation of each configuration (i.e. $\sim 040^\circ$ for AUSMEX, 050° for
567 AUSWUS, 080° for SWEAT and 010° for Missing Link) differs, and by how far north along the Laurentian
568 coast Australia is attached. We find that maximum spreading rates for all configurations occur at 725 Ma,
569 with spreading rate increasing as rifting time decreases due to Australia having to move the same distance, in a
570 shorter time (i.e. 3500 km of spreading in 150 myr, or 75 myr). Similarly, the angular rotation rate is higher
571 because of the shorter time between rifting and 650 Ma. Coupled with changes in rifting times, we can see that
572 the reconstruction with the highest angular rotation is SWEAT at 725 Ma, while the reconstruction with the
573 lowest angular rotation is AUSMEX at 800 Ma. Given modern day limits on spreading rates and angular
574 rotation (e.g. Bird 2003; Zahirovic et al. 2015), either an AUSWUS or AUSMEX configuration with rifting at
575 800 Ma is, kinematically, the most optimal configuration, though SWEAT at 800 Ma could be permissible,
576 though the spreading rate would be just over the upper limit of modern day acceptability. Later rifting times
577 for all configurations must account for the higher spreading rate, and rifting at either 750 Ma or 725 Ma must
578 also account for high rates of angular rotation. Later rifting times also create a limit on the size of the Paleo-
579 pacific ocean, even permitting faster spreading rates (120-140 mm/yr), the maximum basin width is limited to
580 ~ 3500 km (between Mawson and Laurentia, equivalent to 10000 km of seafloor spreading). A global

581 reconstruction would necessitate having a wide enough ocean basin to allow for both Amazonia and West
582 Africa to slip past southern Gondwana (along the Transbrasiliano lineament?). Earlier rifting times between
583 Australia and Laurentia can accommodate larger basin sizes while maintaining reasonable rifting rates.

584

585 Convergence rates for India's motion into Gondwana are also within present day limits and bear similarity
586 with the present day convergence rates of India and Eurasia. The slow down at 650 Ma of India relative to
587 Congo is likely related to the tectonic configuration between it and Congo during this time, where, a series of
588 terranes (e.g. Azania) were being accreted to the Congo margin prior to India's arrival. Closure of a backarc
589 basin between Azania and Congo between 650-580 Ma (Collins and Pisarevsky 2005), or double dipping
590 subduction of the Mozambique ocean under Azania, along with subduction under Congo closing the back-arc
591 basin (Plavsa et al. 2014), are similar to tectonic models of India-Eurasia convergence today (Jagoutz et al.
592 2015; Van der Voo et al. 1999). Importantly, inferences of India kinematics between the times where its
593 position is known from paleomagnetic data (the Malani Igneous Suite and Bhandar and Rewa Series at 770
594 Ma and ~550 Ma respectively) are reasonable. Assuming a direct interpolation between both poles requires a
595 convergence rate of ~50-70 mm/year. We have followed the idea that India slipped past Australia along a
596 transform boundary, though a range of positions of India at 650 Ma are shown in Figure 9 that satisfy the
597 geological data of its collision with Congo but not necessarily this transform boundary with Australia. If India
598 converges too slowly it is further south than Australia, while high convergence rates create an incredibly large
599 ocean basin that is consumed.

600

601 **Relative plate motion stability**

602

603 The orientation of spreading systems for AUSMEX, AUSWUS and SWEAT configurations is perhaps
604 unrealistic, especially for the older times. Since Pangea breakup, every major ocean basin (Atlantic, Indian,
605 Pacific) has experienced reorganisation events of varying magnitudes (Müller et al. 2016). Changes in plate
606 kinematics are obviously not captured in the simpler reconstruction cases, which exhibit a first order pattern
607 similar to an Atlantic-type basin opening. We would expect that post Australia-Laurentia rifting, other
608 constituents of western Rodinia also begin to separate (e.g. Congo-São Francisco at ~750 Ma, Kalahari at

609 ~700 Ma; Jacobs et al. 2008; Li et al. 2008) leading to new MOR complexes and the potential for
610 reorganisation events that would impact the Australia-Laurentia MOR. Ideally, complete plate models (i.e.
611 continents and plate boundaries) for the Neoproterozoic can be used to help constrain possible motions and
612 configurations.

613

614 The more complex flowlines and series of Euler Poles for the Missing-Link Model, compared with the
615 relatively smooth flowlines of the other three models, are a function for the motions of Australia and South
616 China relative to Laurentia implemented in this model. They explain the motion of South China northwards
617 from the Australia-Laurentia nexus, and then westwards over Australia, and then southwards down the west
618 coast of Australia for Gondwana amalgamation, while Australia is also rifting westwards from Laurentia (Li
619 et al. 2008; 2013). This more complex motion necessitates several major changes in angular rotation, mid-
620 ocean ridge orientations and spreading rates. The movement of Australia relative to Laurentia is similar to
621 that of SWEAT, as Australia is located in a similar position relative to the Laurentian coastline, though it is
622 more upright (N-S orientated), which has the effect of reducing both its spreading rate and angular rotation
623 (when compared to SWEAT), and would create an even more kinematically conservative rifting pattern than
624 AUSWUS or AUSMEX.

625

626 A potential solution to account for the motion of South China in the Missing Link Model could follow the
627 suggestion of Cawood et al. (2013), where the Yangtze Block of South China represents an early
628 Neoproterozoic accretionary complex growing on the north side of the Cathaysia craton. This would suggest
629 that South China was yet to be fully cratonised and potentially lack a deep cratonic root, allowing for more
630 rapid and diverse motions than what we would expect using cratonic crust in the present day. Additionally,
631 following the reasoning behind the Missing-Link model, the presence of a plume head (Li et al. 1999) could
632 help facilitate more rapid and diverse motions as well through decoupling from the underlying mantle (e.g.
633 Ratcliff et al. 1998). A similar exposition of plate motions could be found in the tectonic evolution of the
634 Southeast Asia over the last ~150 Myr, where periodic rifting of small terranes and continental slithers during
635 the Mesozoic from the northern Gondwanian margin to the southern Eurasian margin, has, in part, resulted in

636 a complex melangé of terranes, seafloor spreading complexes, extinct ridges, subduction zones and changes in
637 plate motion (e.g. Metcalfe 1996; 2011; Zahirovic et al. 2014).

638

639 **Integration of kinematic observations**

640

641 By integrating both sets of kinematic observations, along with the motion of two (poorly constrained) cratons,
642 Congo-São Francisco (C-SF) and Kalahari, we can build a quantitative relative plate model bounded by
643 absolute plate positions and constrained by geology. Following Li et al. (2008), but acknowledging the wide
644 array of ideas about the Neoproterozoic journeys of C-SF and Kalahari (e.g. Evans 2009; Frimmel et al. 2011;
645 Johnson et al. 2005; McGee et al. 2012; Wingate et al. 2010), we take the AUSWUS fit with rifting at 800 Ma
646 (Fig. 10a), C-SF-Laurentia rifting at 750 Ma (McGee et al. 2012) (Fig. 10b) and Kalahari-Laurentia rifting at
647 700 Ma (Fig. 10c,d). Based on the maximum expected spreading rate of Australia rifting from Laurentia at
648 800 Ma, we see a configuration with Australia and Kalahari with $\sim 15^\circ$ of latitude and longitude separation,
649 but otherwise in a position favourable with what we expect for Gondwana amalgamation. Following the
650 present day development of ocean basins (e.g. East Gondwana breakup), we interpret that the new spreading
651 system between Laurentia-Kalahari at 700 Ma is most likely to be an extension of the existing one between
652 Australia-Laurentia, either rifting in the same direction as Australia, or causing a reorganisation and altering
653 the divergence direction such that while there is some minor relative motion between Australia-Kalahari (to
654 accommodate the 650 Ma YF pole), they are otherwise moving on the same longitude. Given the lack of
655 paleomagnetic data from the Kalahari Craton, it is impossible to constrain its position until ~ 550 Ma when it
656 collides with Congo forming the Damara–Lufilian–Zambezi Orogen (Johnson et al. 2005), at which point it
657 ‘paleomagnetically reappears’, using the Gondwana APWP, at mid-latitudes (Torsvik et al. 2012). This is
658 more southerly than it’s (inferred) rifting position from Laurentia, suggesting that it’s relative motion can’t be
659 aligned with orientation of Australia-Laurentia spreading system (Fig. 10c), rather there is a reorganisation,
660 changing the orientation of Australia-Laurentia rifting (Fig. 10d). We express this relative motion by a stage
661 rotation of Australia relative to Congo around the Euler Pole $-5^\circ S -98^\circ W$ 57° .

662

663 By 650 Ma, India is starting its (plotted) southward descent into Gondwana around the Euler Pole $11^{\circ}N$ $59^{\circ}E$ -
664 72° (Fig. 10e,f). The position of Australia can be constrained well now, due to paleomagnetic data, and we see
665 that the conjunction of the absolute latitudinal position of Australia, along with geological data, fit well with
666 the relative motions of the Indian plate to both Australia and Congo, with India moving past Australia along a
667 transform fault (Fig. 10f). The rotation of Australia into Gondwana is more uncertain, primarily because of
668 the lack of data from Antarctica, which forms the nucleus of eastern Gondwana amalgamation (e.g. An et al.
669 2015; Boger 2011). Both the Coats Land Block (colliding with Dronning Maud Land in Kalahari at 560 Ma
670 after Boger (2011), and the hypothesized Crohn Craton (Boger 2011) act as an extension of the Mawson
671 Craton (perhaps as series of accreted terranes?) and are the precursor to Australia–East-Antarctica’s collision,
672 which is likely to have occurred along a suture represented by the East-Antarctica Mountain Ranges
673 (EAMOR) (An et al. 2015). The high quality poles from the Lower Arumbera and Upper Pertatataka
674 Formations at ~ 540 Ma (Kirschvink, 1978) constrain Australia to a position where it’s movement into
675 Gondwana is head on into India along the Kuungan orogeny (Meert 2003; Meert and Van der Voo 1997),
676 with a strike-slip motion along the Coats Land Block (Fig. 10g,h). This is perhaps somewhat supported by the
677 granulite facies along the Kuungan orogeny suggesting a major collisional event (e.g. Kelsey et al. 2007;
678 Grantham et al, 2013), though we note that future data from Antarctica may cause this to be revised. The
679 motion of Australia–East-Antarctica relative to Congo is defined by the Euler Pole $-38^{\circ}S$ $-75^{\circ}W$ 40° .

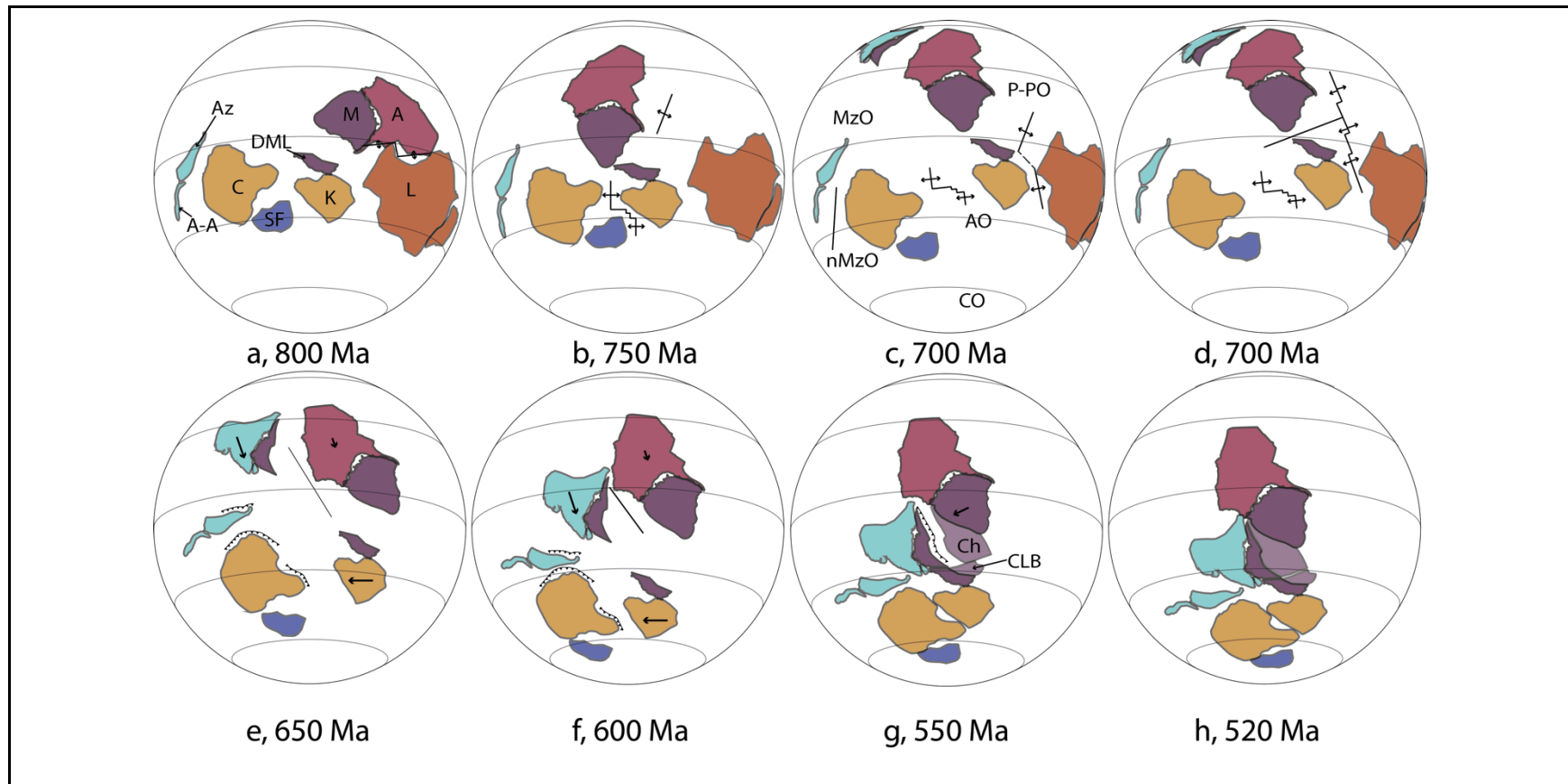


Figure 11: Reconstruction incorporating breakup of western Rodinia and amalgamation of Eastern Gondwana. Two possible options of spreading ridges at 700 Ma (when Kalahari rifts from Laurentia) either having divergence between Australia-Kalahari (c), or both moving along the same longitude (d). AO, Adamastor Ocean; CO, Clymene Ocean; MzO, Mozambique Ocean; nMzO, Neomozambique Ocean; P-PO, Paleo-Pacific Ocean.

See Figure 9 for other label details.

682

683 **Non-unique solutions**

684

685 The (rudimentary) model described above is a non-unique solution of the Rodinia-Gondwana transition.
686 Variations in Australia-Laurentia configurations can change interpretations about spreading systems in late-
687 stage Rodinia breakup, particularly with respect to the position of South China. Changes in rifting time of this
688 configuration will also strongly alter both the kinematics (if one desires Australia to be in the position
689 described above) and development of spreading systems during late-stage Rodinia rifting when considering the
690 other cratonic components (e.g. Kalahari, C-SF, Rio de la Plata). We also sidestep the problem of India's
691 position (and inclusion) in Rodinia, noting that its 700 Ma position would be similar for models with India
692 separate from Rodinia or as a product of early rifting, and that its final position in Gondwana is well
693 established (e.g. Collins and Pisarevsky 2005; Meert et al. 2003). Rather, the emphasis here is on how
694 kinematic tools and data can help users make educated, quantitative decisions about relative plate motions in
695 deep time, especially when there is limited paleomagnetic data (e.g. either a begin or end position/time is well
696 constrained, but the other is not). We also stress that decisions about the distances that plates move in a given
697 model carry implications for mantle processes and geodynamics. For example, the maximum convergence
698 rate of India-Congo from 700-550 Ma necessitates the closure of a ~14000 km wide ocean basin. The
699 implication of a large slab burial ground (as compared to a slower convergence model which results in less
700 subducted oceanic crust) is a strong drawdown effect of any overlaying portions of continental crust,
701 potentially preserving a dynamic topography signature within sedimentary basins (e.g. Flowers et al. 2012).

702

703 **Conclusions**

704

705 Kinematic data suggest that a tectonic model where Rodinia splits up before 750 Ma is more consistent with
706 Phanerozoic plate tectonics than competing models, in that an early split-up minimises both the speed and
707 angular rotation of the Australian Plate, with rifting at ca. 800 Ma producing the only models that are within
708 Phanerozoic spreading rate limits. SWEAT, AUSWUS and AUSMEX all have similar maximum rates of
709 angular rotation (~1.9°/Myr at 725 Ma), though the SWEAT configuration has the highest average spreading

710 rate for all rifting times (149 mm/yr at 725 Ma rifting). AUSWUS has the lowest average spreading rates (56
711 mm/yr at 800 Ma rifting), though AUSMEX is only slightly faster at 64 mm/yr. Kinematically, AUSWUS
712 and AUSMEX at 800 Ma are the two preferred rifting configurations/times, though SWEAT at 800 Ma could
713 be justifiable (76 mm/yr maximum spreading rate). As the onset of rifting becomes younger, the viability of
714 configurations decreases due to the corresponding increase in subsequent spreading rates. For a rifting time of
715 725 Ma for any configuration, viable reasons for spreading rates of greater than 130 mm/yr would have to be
716 provided. Similarly, for the Missing-Link Model, rifting at 800 Ma presents the most optimal spreading rates,
717 though the flowlines and spikes in spreading rate and angular rotation for South China require a more
718 complex explanation than that of the other configurations. We also demonstrate how kinematic tools can help
719 constrain relative plate motions by creating a simple model that explicitly links together paleomagnetic,
720 geological and kinematic data to explain the relative motions of India to Congo and Australia during its
721 collision with Gondwana.

722

723

724 **Acknowledgements**

725

726 This manuscript is a contribution to IGCP 648, Supercontinent Cycles and Global Geodynamics. This
727 research was supported by the Science Industry Endowment Fund (RP 04-174) Big Data Knowledge
728 Discovery Project. ASM is supported by the CSIRO-Data61 Postgraduate Scholarships.

729

730 **Supplementary Material**

731

732 Supplementary material is downloadable following this link:

733

734 <https://cloudstor.aarnet.edu.au/plus/index.php/s/2kKJUB5GOpNhICK>

735

736 (Expiry date: 31/10/2016)

737

738 **References**

739

- 740 1. An, M., Wiens, D.A., Zhao, Y., Feng, M., Nyblade, A.A., Kanao, M., Li, Y., Maggi, A. and
741 Lévêque, J.J., 2015. S-velocity model and inferred Moho topography beneath the Antarctic Plate from
742 Rayleigh waves. *Journal of Geophysical Research: Solid Earth*, 120(1), pp.359-383.
- 743 2. Archibald, D.B., Collins, A.S., Foden, J.D., Payne, J.L., Taylor, R., Holden, P., Razakamanana, T.
744 and Clark, C., 2015. Towards unravelling the Mozambique Ocean conundrum using a triumvirate of
745 zircon isotopic proxies on the Ambatolampy Group, central Madagascar. *Tectonophysics*, 662, pp.167-
746 182.
- 747 3. Argus, D.F., Gordon, R.G. and DeMets, C., 2011. Geologically current motion of 56 plates relative
748 to the no-net-rotation reference frame. *Geochemistry, Geophysics, Geosystems*, 12(11).
- 749 4. Argus, D.F., Gordon, R.G., Heflin, M.B., Ma, C., Eanes, R.J., Willis, P., Peltier, W.R. and Owen,
750 S.E., 2010. The angular velocities of the plates and the velocity of Earth's centre from space geodesy.
751 *Geophysical Journal International*, 180(3), pp.913-960.
- 752 5. Ashwal, L.D., Hamilton, M.A., Morel, V.P. and Rabeloson, R.A., 1998. Geology, petrology and
753 isotope geochemistry of massif-type anorthosites from southwest Madagascar. *Contributions to
754 Mineralogy and Petrology*, 133(4), pp.389-401.
- 755 6. Austermann, J., Ben-Avraham, Z., Bird, P., Heidbach, O., Schubert, G. and Stock, J.M., 2011.
756 Quantifying the forces needed for the rapid change of Pacific plate motion at 6Ma. *Earth and Planetary
757 Science Letters*, 307(3), pp.289-297.
- 758 7. Bell, R.T. and Jefferson, C.W., 1987. An hypothesis for an Australian-Canadian connection in the
759 Late Proterozoic and the birth of the Pacific Ocean. In *Proceedings, Pacific Rim Congress* (Vol. 87, pp.
760 39-50).
- 761 8. Bierlein, F.P., Groves, D.I. and Cawood, P.A., 2009. Metallogeny of accretionary orogens—the
762 connection between lithospheric processes and metal endowment. *Ore Geology Reviews*, 36(4), pp.282-
763 292.
- 764 9. Bird, P., 2003. An updated digital model of plate boundaries. *Geochemistry, Geophysics, Geosystems*,
765 4(3).
- 766 10. Boger, S.D., 2011. Antarctica—before and after Gondwana. *Gondwana Research*, 19(2), pp.335-371.

- 767 11. Boger, S.D., Hirdes, W., Ferreira, C.A.M., Jenett, T., Dallwig, R. and Fanning, C.M., 2015. The
768 580–520Ma Gondwana suture of Madagascar and its continuation into Antarctica and Africa.
769 *Gondwana Research*, 28(3), pp.1048-1060.
- 770 12. Borg, S.G. and DePaolo, D.J., 1994. Laurentia, Australia, and Antarctica as a Late Proterozoic
771 supercontinent: constraints from isotopic mapping. *Geology*, 22(4), pp.307-310.
- 772 13. Bradley, D.C., 2011. Secular trends in the geologic record and the supercontinent cycle. *Earth-Science*
773 *Reviews*, 108(1), pp.16-33.
- 774 14. Brasier, M.D. and Lindsay, J.F., 2001. Did supercontinental amalgamation trigger the “Cambrian
775 Explosion”. *The Ecology of the Cambrian Radiation*. Columbia University Press, New York, pp.69-89.
- 776 15. Brookfield, M.E., 1993. Neoproterozoic Laurentia-Australia fit. *Geology*, 21(8), pp.683-686.
- 777 16. Buchwaldt, R., Tucker, R.D. and Dymek, R.F., 2003. Geothermobarometry and U-Pb
778 Geochronology of metapelitic granulites and pelitic migmatites from the Lokoho region, Northern
779 Madagascar. *American Mineralogist*, 88(11-12), pp.1753-1768.
- 780 17. Burrett, C. and Berry, R., 2000. Proterozoic Australia–Western United States (AUSWUS) fit between
781 Laurentia and Australia. *Geology*, 28(2), pp.103-106.
- 782 18. Burrett, C. and Berry, R., 2002. A Statistical Approach to Defining Proterozoic Crustal Provinces and
783 Testing Continental Reconstructions of Australia and Laurentia-SWEAT or AUSWUS?. *Gondwana*
784 *Research*, 5(1), pp.109-122.
- 785 19. Butterworth, N.P., Talsma, A.S., Müller, R.D., Seton, M., Bunge, H.P., Schuberth, B.S.A.,
786 Shephard, G.E. and Heine, C., 2014. Geological, tomographic, kinematic and geodynamic
787 constraints on the dynamics of sinking slabs. *Journal of Geodynamics*, 73, pp.1-13.
- 788 20. Cande, S.C. and Patriat, P., 2015. The anticorrelated velocities of Africa and India in the Late
789 Cretaceous and early Cenozoic. *Geophysical Journal International*, 200(1), pp.227-243.
- 790 21. Cande, S.C. and Stegman, D.R., 2011. Indian and African plate motions driven by the push force of
791 the Reunion plume head. *Nature*, 475(7354), pp.47-52.
- 792 22. Cawood, P.A. and Buchan, C., 2007. Linking accretionary orogenesis with supercontinent assembly.
793 *Earth-Science Reviews*, 82(3), pp.217-256.

- 794 23. Cawood, P.A., Wang, Y., Xu, Y. and Zhao, G., 2013. Locating South China in Rodinia and
795 Gondwana: A fragment of greater India lithosphere?. *Geology*, 41(8), pp.903-906.
- 796 24. Cocks, L.R.M. and Torsvik, T.H., 2002. Earth geography from 500 to 400 million years ago: a faunal
797 and palaeomagnetic review. *Journal of the Geological Society*, 159(6), pp.631-644.
- 798 25. Collins, A.S., 2003. Structure and age of the northern Leeuwin Complex, Western Australia:
799 constraints from field mapping and U–Pb isotopic analysis. *Australian Journal of Earth Sciences*, 50(4),
800 pp.585-599.
- 801 26. Collins, A.S., 2006. Madagascar and the amalgamation of Central Gondwana. *Gondwana Research*,
802 9(1), pp.3-16.
- 803 27. Collins, A.S., Clark, C. and Plavsa, D., 2014. Peninsular India in Gondwana: the tectonothermal
804 evolution of the Southern Granulite Terrain and its Gondwanan counterparts. *Gondwana Research*,
805 25(1), pp.190-203.
- 806 28. Collins, A.S., Clark, C., Sajeev, K., Santosh, M., Kelsey, D.E. and Hand, M., 2007. Passage through
807 India: the Mozambique Ocean suture, high-pressure granulites and the Palghat-Cauvery shear zone
808 system. *Terra Nova*, 19(2), pp.141-147.
- 809 29. Collins, A.S. and Pisarevsky, S.A., 2005. Amalgamating eastern Gondwana: the evolution of the
810 Circum-Indian Orogens. *Earth-Science Reviews*, 71(3), pp.229-270.
- 811 30. Condie, K.C., Belousova, E., Griffin, W.L. and Sircombe, K.N., 2009. Granitoid events in space and
812 time: constraints from igneous and detrital zircon age spectra. *Gondwana Research*, 15(3), pp.228-242.
- 813 31. Dalziel, I.W., 1991. Pacific margins of Laurentia and East Antarctica-Australia as a conjugate rift
814 pair: Evidence and implications for an Eocambrian supercontinent. *Geology*, 19(6), pp.598-601.
- 815 32. Davidson, A., 2008. Late Paleoproterozoic to mid-Neoproterozoic history of northern Laurentia: an
816 overview of central Rodinia. *Precambrian Research*, 160(1), pp.5-22.
- 817 33. Denyszyn, S.W., Halls, H.C., Davis, D.W. and Evans, D.A., 2009. Paleomagnetism and U-Pb
818 geochronology of Franklin dykes in High Arctic Canada and Greenland: a revised age and
819 paleomagnetic pole constraining block rotations in the Nares Strait region. *Canadian Journal of Earth
820 Sciences*, 46(9), pp.689-705.

- 821 34. Domeier, M., 2015. A plate tectonic scenario for the Iapetus and Rheic oceans. *Gondwana Research*,
822 36, pp.275-295.
- 823 35. Domeier, M. and Torsvik, T.H., 2014. Plate tectonics in the late Paleozoic. *Geoscience Frontiers*, 5(3),
824 pp.303-350.
- 825 36. Du, L., Guo, J., Nutman, A.P., Wyman, D., Geng, Y., Yang, C., Liu, F., Ren, L. and Zhou, X.,
826 2014. Implications for Rodinia reconstructions for the initiation of Neoproterozoic subduction at~
827 860Ma on the western margin of the Yangtze Block: Evidence from the Guandaoshan Pluton. *Lithos*,
828 196, pp.67-82.
- 829 37. Eisbacher, G.H., 1985. Late Proterozoic rifting, glacial sedimentation, and sedimentary cycles in the
830 light of Windermere deposition, western Canada. *Palaeogeography, Palaeoclimatology, Palaeoecology*,
831 51(1-4), pp.231-254.
- 832 38. Embleton, B.J.J. and Schmidt, P.W., 1985. Age and significance of magnetizations in dolerite dykes
833 from the Northampton Block, Western Australia. *Australian Journal of Earth Sciences*, 32(3), pp.279-286.
- 834 39. Ernst, R. and Bleeker, W., 2010. Large igneous provinces (LIPs), giant dyke swarms, and mantle
835 plumes: significance for breakup events within Canada and adjacent regions from 2.5 Ga to the
836 Present. *Canadian Journal of Earth Sciences*, 47(5), pp.695-739.
- 837 40. Ernst, R.E., Bleeker, W., Söderlund, U. and Kerr, A.C., 2013. Large Igneous Provinces and
838 supercontinents: Toward completing the plate tectonic revolution. *Lithos*, 174, pp.1-14.
- 839 41. Ernst, R.E., Wingate, M.T.D., Buchan, K.L. and Li, Z.X., 2008. Global record of 1600–700Ma Large
840 Igneous Provinces (LIPs): implications for the reconstruction of the proposed Nuna (Columbia) and
841 Rodinia supercontinents. *Precambrian Research*, 160(1), pp.159-178.
- 842 42. Evans, D.A., 2009. The palaeomagnetically viable, long-lived and all-inclusive Rodinia
843 supercontinent reconstruction. *Geological Society, London, Special Publications*, 327(1), pp.371-404.
- 844 43. Fitzsimons, I.C.W., 2000. Grenville-age basement provinces in East Antarctica: evidence for three
845 separate collisional orogens. *Geology*, 28(10), pp.879-882.
- 846 44. Fitzsimons, I.C.W., 2003. Proterozoic basement provinces of southern and southwestern Australia,
847 and their correlation with Antarctica. *Geological Society, London, Special Publications*, 206(1), pp.93-130.

- 848 45. Fitzsimons, I.C., 2016. Pan–African granulites of Madagascar and southern India: Gondwana
849 assembly and parallels with modern Tibet. *Journal of Mineralogical and Petrological Sciences*, 111(2),
850 pp.73-88.
- 851 46. Flowers, R.M., Ault, A.K., Kelley, S.A., Zhang, N. and Zhong, S., 2012. Epeirogeny or eustasy?
852 Paleozoic–Mesozoic vertical motion of the North American continental interior from
853 thermochronometry and implications for mantle dynamics. *Earth and Planetary Science Letters*, 317,
854 pp.436-445.
- 855 47. Frimmel, H.E., Basei, M.S. and Gaucher, C., 2011. Neoproterozoic geodynamic evolution of SW-
856 Gondwana: a southern African perspective. *International Journal of Earth Sciences*, 100(2-3), pp.323-354.
- 857 48. Ganade, C.E., Cordani, U.G., Agbossoumounde, Y., Caby, R., Basei, M.A., Weinberg, R.F. and
858 Sato, K., 2016. Tightening-up NE Brazil and NW Africa connections: New U–Pb/Lu–Hf zircon data
859 of a complete plate tectonic cycle in the Dahomey belt of the West Gondwana Orogen in Togo and
860 Benin. *Precambrian Research*, 276, pp.24-42.
- 861 49. Gernon, T.M., Hincks, T.K., Tyrrell, T., Rohling, E.J. and Palmer, M.R., 2016. Snowball Earth
862 ocean chemistry driven by extensive ridge volcanism during Rodinia breakup. *Nature Geoscience*, 9(3),
863 pp.242-248.
- 864 50. Goodge, J.W., Vervoort, J.D., Fanning, C.M., Brecke, D.M., Farmer, G.L., Williams, I.S., Myrow,
865 P.M. and DePaolo, D.J., 2008. A positive test of East Antarctica–Laurentia juxtaposition within the
866 Rodinia supercontinent. *Science*, 321(5886), pp.235-240.
- 867 51. Groves, D.I., Goldfarb, R.J., Gebre-Mariam, M., Hagemann, S.G. and Robert, F., 1998. Orogenic
868 gold deposits: a proposed classification in the context of their crustal distribution and relationship to
869 other gold deposit types. *Ore geology reviews*, 13(1), pp.7-27.
- 870 52. Halverson, G.P., Hurtgen, M.T., Porter, S.M. and **Collins, A.S.** 2009. Neoproterozoic-Cambrian
871 Biogeochemical Evolution. In C. Gaucher, A.N. Sial, G.P. Halverson, and H.E. Frimmel (Eds.).
872 *Neoproterozoic-Cambrian Tectonics, Global Change and Evolution: a focus on southwestern Gondwana*.
873 Developments in Precambrian Geology, Volume 16, Elsevier, pp.351-365.

- 874 53. Harlan, S.S., Geissman, J.W. and Snee, L.W., 1997. *Paleomagnetic and $^{40}\text{Ar}/^{39}\text{Ar}$ geochronologic data*
875 *from late Proterozoic mafic dikes and sills, Montana and Wyoming* (p. 1580). US Government Printing
876 Office.
- 877 54. Harris, L.B., 1994. Neoproterozoic sinistral displacement along the Darling mobile belt, Western
878 Australia, during Gondwanaland assembly. *Journal of the Geological Society*, 151(6), pp.901-904.
- 879 55. Harris, L.B. and Beeson, J., 1993. Gondwanaland significance of Lower Palaeozoic deformation in
880 central India and SW Western Australia. *Journal of the Geological Society*, 150(5), pp.811-814.
- 881 56. Hoffman, P.F., 1991. Did the breakout of Laurentia turn Gondwanaland inside-out. *Science*,
882 252(5011), pp.1409-1412.
- 883 57. Hoffman, P.F. and Li, Z.X., 2009. A palaeogeographic context for Neoproterozoic glaciation.
884 *Palaeogeography, Palaeoclimatology, Palaeoecology*, 277(3), pp.158-172.
- 885 58. Iaffaldano, G., Bunge, H.P. and Dixon, T.H., 2006. Feedback between mountain belt growth and
886 plate convergence. *Geology*, 34(10), pp.893-896.
- 887 59. Jacobs, J., Pisarevsky, S., Thomas, R.J. and Becker, T., 2008. The Kalahari Craton during the
888 assembly and dispersal of Rodinia. *Precambrian Research*, 160(1), pp.142-158.
- 889 60. Jagoutz, O., Royden, L., Holt, A.F. and Becker, T.W., 2015. Anomalously fast convergence of India
890 and Eurasia caused by double subduction. *Nature Geoscience*, 8(6), pp.475-478.
- 891 61. Johansson, Å., 2014. From Rodinia to Gondwana with the 'SAMBA' model—a distant view from
892 Baltica towards Amazonia and beyond. *Precambrian Research*, 244, pp.226-235.
- 893 62. Johnson, S.P., Rivers, T. and De Waele, B., 2005. A review of the Mesoproterozoic to early
894 Palaeozoic magmatic and tectonothermal history of south-central Africa: implications for Rodinia
895 and Gondwana. *Journal of the Geological Society*, 162(3), pp.433-450.
- 896 63. Karlstrom, K.E., Åhäll, K.I., Harlan, S.S., Williams, M.L., McLelland, J. and Geissman, J.W., 2001.
897 Long-lived (1.8–1.0 Ga) convergent orogen in southern Laurentia, its extensions to Australia and
898 Baltica, and implications for refining Rodinia. *Precambrian Research*, 111(1), pp.5-30.
- 899 64. Karlstrom, K.E., Williams, M.L., McLelland, J., Geissman, J.W. and Ahall, K., 1999. Refining
900 Rodinia: geologic evidence for the Australia-Western US connection in the Proterozoic. *GSA Today*,
901 9(10), pp.2-6

- 902 65. Kelsey, D.E., Hand, M., Clark, C. and Wilson, C.J.L., 2007. On the application of in situ monazite
903 chemical geochronology to constraining P–T–t histories in high-temperature (> 850° C)
904 polymetamorphic granulites from Prydz Bay, East Antarctica. *Journal of the Geological Society*, 164(3),
905 pp.667-683.
- 906 66. King, S.D., Lowman, J.P. and Gable, C.W., 2002. Episodic tectonic plate reorganizations driven by
907 mantle convection. *Earth and Planetary Science Letters*, 203(1), pp.83-91.
- 908 67. Kirschvink, J.L., 1978. The Precambrian-Cambrian boundary problem: Paleomagnetic directions
909 from the Amadeus basin, central Australia. *Earth and Planetary Science Letters*, 40(1), pp.91-100.
- 910 68. Knesel, K.M., Cohen, B.E., Vasconcelos, P.M. and Thiede, D.S., 2008. Rapid change in drift of the
911 Australian plate records collision with Ontong Java plateau. *Nature*, 454(7205), pp.754-757.
- 912 69. Li, Z.X., 2000. New palaeomagnetic results from the ‘cap dolomite’ of the Neoproterozoic Walsh
913 Tillite, northwestern Australia. *Precambrian Research*, 100(1), pp.359-370.
- 914 70. Li, Z., Qiu, N., Chang, J. and Yang, X., 2015. Precambrian evolution of the Tarim Block and its
915 tectonic affinity to other major continental blocks in China: New clues from U–Pb geochronology and
916 Lu–Hf isotopes of detrital zircons. *Precambrian Research*, 270, pp.1-21.
- 917 71. Li, Z.X. and Evans, D.A., 2011. Late Neoproterozoic 40 intraplate rotation within Australia allows
918 for a tighter-fitting and longer-lasting Rodinia. *Geology*, 39(1), pp.39-42.
- 919 72. Li, Z.X., Bogdanova, S.V., Collins, A.S., Davidson, A., De Waele, B., Ernst, R.E., Fitzsimons,
920 I.C.W., Fuck, R.A., Gladkochub, D.P., Jacobs, J. and Karlstrom, K.E., 2008. Assembly,
921 configuration, and break-up history of Rodinia: a synthesis. *Precambrian research*, 160(1), pp.179-210.
- 922 73. Li, Z.X., Evans, D.A. and Halverson, G.P., 2013. Neoproterozoic glaciations in a revised global
923 palaeogeography from the breakup of Rodinia to the assembly of Gondwanaland. *Sedimentary Geology*,
924 294, pp.219-232.
- 925 74. Li, Z.X., Li, X.H., Kinny, P.D. and Wang, J., 1999. The breakup of Rodinia: did it start with a
926 mantle plume beneath South China?. *Earth and Planetary Science Letters*, 173(3), pp.171-181.
- 927 75. Li, Z.X., Zhang, L. and Powell, C.M., 1995. South China in Rodinia: part of the missing link between
928 Australia–East Antarctica and Laurentia?. *Geology*, 23(5), pp.407-410.

- 929 76. Lowman, J.P., King, S.D. and Gable, C.W., 2003. The role of the heating mode of the mantle in
930 intermittent reorganization of the plate velocity field. *Geophysical Journal International*, 152(2), pp.455-
931 467.
- 932 77. Maruyama, S. and Santosh, M., 2008. Models on Snowball Earth and Cambrian explosion: A
933 synopsis. *Gondwana Research*, 14(1), pp.22-32.
- 934 78. Matthews, K.J., Müller, R.D., Wessel, P., and Whittaker, J.M., 2011. The tectonic fabric of the ocean
935 basins. *Journal of Geophysical Research: Solid Earth*, 116(B12).
- 936 79. Matthews, K.J., Seton, M. and Müller, R.D., 2012. A global-scale plate reorganization event at 105-
937 100Ma. *Earth and Planetary Science Letters*, 355, pp.283-298.
- 938 80. McElhinny, M.W., Cowley, J.A. and Edwards, D.J., 1978. Palaeomagnetism of some rocks from
939 Peninsular India and Kashmir. *Tectonophysics*, 50(1), pp.41-54.
- 940 81. McGee, B., Halverson, G.P. and Collins, A.S., 2012. Cryogenian rift-related magmatism and
941 sedimentation: South-western Congo Craton, Namibia. *Journal of African Earth Sciences*, 76, pp.34-49.
- 942 82. Meert, J.G., 2002. Paleomagnetic evidence for a Paleo-Mesoproterozoic supercontinent Columbia.
943 *Gondwana Research*, 5(1), pp.207-215.
- 944 83. Meert, J.G., 2003. A synopsis of events related to the assembly of eastern Gondwana. *Tectonophysics*,
945 362(1), pp.1-40.
- 946 84. Meert, J.G. and Lieberman, B.S., 2008. The Neoproterozoic assembly of Gondwana and its
947 relationship to the Ediacaran–Cambrian radiation. *Gondwana Research*, 14(1), pp.5-21.
- 948 85. Meert, J.G. and Torsvik, T.H., 2003. The making and unmaking of a supercontinent: Rodinia
949 revisited. *Tectonophysics*, 375(1), pp.261-288.
- 950 86. Meert, J.G. and Van Der Voo, R., 1997. The assembly of Gondwana 800-550 Ma. *Journal of*
951 *Geodynamics*, 23(3), pp.223-235.
- 952 87. Metcalfe, I., 1996. Pre-Cretaceous evolution of SE Asian terranes. *Geological Society, London, Special*
953 *Publications*, 106(1), pp.97-122.
- 954 88. Metcalfe, I., 2011. Tectonic framework and Phanerozoic evolution of Sundaland. *Gondwana Research*,
955 19(1), pp.3-21.

- 956 89. Moores, E.M., 1991. Southwest US-East Antarctic (SWEAT) connection: a hypothesis. *Geology*,
957 19(5), pp.425-428.
- 958 90. Morgan, W.J., 1971. Convection plumes in the lower mantle. *Nature*, 230, pp.42-43.
- 959 91. Mulder, J.A., Halpin, J.A. and Daczko, N.R., 2015. Mesoproterozoic Tasmania: Witness to the East
960 Antarctica–Laurentia connection within Nuna. *Geology*, 43(9), pp.759-762.
- 961 92. Müller, R.D., Royer, J.Y. and Lawver, L.A., 1993. Revised plate motions relative to the hotspots
962 from combined Atlantic and Indian Ocean hotspot tracks. *Geology*, 21(3), pp.275-278.
- 963 93. Müller, R.D., Seton, M., Zahirovic, S., Williams, S.E., Matthews, K.J., Wright, N.M., Shephard,
964 G.E., Maloney, K., Barnett-Moore, N., Hosseinpour, M. and Bower, D.J., 2016. Ocean basin
965 evolution and global-scale plate reorganization events since Pangea breakup. *Annual Review of Earth
966 and Planetary Sciences*, 44(1), pp.107-138.
- 967 94. Murthy, G., Gower, C., Tubrett, M. and Pätzold, R., 1992. Paleomagnetism of Eocambrian Long
968 Range dykes and Double Mer Formation from Labrador, Canada. *Canadian Journal of Earth Sciences*,
969 29(6), pp.1224-1234.
- 970 95. Nance, R.D. and Murphy, J.B., 2013. Origins of the supercontinent cycle. *Geoscience Frontiers*, 4(4),
971 pp.439-448.
- 972 96. Nance, R.D., Murphy, J.B. and Santosh, M., 2014. The supercontinent cycle: a retrospective essay.
973 *Gondwana Research*, 25(1), pp.4-29.
- 974 97. Palmer, H.C., Merz, B.A. and Hayatsu, A., 1977. The Sudbury dikes of the Grenville Front region:
975 paleomagnetism, petrochemistry, and K-Ar age studies. *Canadian Journal of Earth Sciences*, 14(8),
976 pp.1867-1887.
- 977 98. Park, J.K., Norris, D.K. and Larochelle, A., 1989. Paleomagnetism and the origin of the Mackenzie
978 Arc of northwestern Canada. *Canadian Journal of Earth Sciences*, 26(11), pp.2194-2203.
- 979 99. Patriat, P. and Achache, J., 1984. India–Eurasia collision chronology has implications for crustal
980 shortening and driving mechanism of plates.
- 981 100. Pehrsson, S.J., Eglington, B.M., Evans, D.A., Huston, D. and Reddy, S.M., 2016.
982 Metallogeny and its link to orogenic style during the Nuna supercontinent cycle. *Geological Society,
983 London, Special Publications*, 424(1), pp.83-94.

- 984 101. Pisarevsky, S.A., Elming, S.Å., Pesonen, L.J. and Li, Z.X., 2014. Mesoproterozoic
985 paleogeography: supercontinent and beyond. *Precambrian Research*, 244, pp.207-225.
- 986 102. Pisarevsky, S.A., Wingate, M.T.D. and Harris, L.B., 2003. Late Mesoproterozoic (ca 1.2 Ga)
987 palaeomagnetism of the Albany–Fraser orogen: no pre-Rodinia Australia–Laurentia connection.
988 *Geophysical Journal International*, 155(1), pp.F6-F11.
- 989 103. Pisarevsky, S.A., Wingate, M.T., Li, Z.X., Wang, X.C., Tohver, E. and Kirkland, C.L.,
990 2014. Age and paleomagnetism of the 1210 Ma Gnowangerup–Fraser dyke swarm, Western
991 Australia, and implications for late Mesoproterozoic paleogeography. *Precambrian Research*, 246, pp.1-
992 15.
- 993 104. Pisarevsky, S.A., Wingate, M.T.D., Stevens, M.K. and Haines, P.W., 2007. Palaeomagnetic
994 results from the Lancer 1 stratigraphic drillhole, Officer Basin, Western Australia, and implications
995 for Rodinia reconstructions. *Australian Journal of Earth Sciences*, 54(4), pp.561-572.
- 996 105. Plavsa, D., Collins, A.S., Payne, J.L., Foden, J.D., Clark, C. and Santosh, M., 2014. Detrital
997 zircons in basement metasedimentary protoliths unveil the origins of southern India. *Geological Society
998 of America Bulletin*, 126(5-6), pp.791-811.
- 999 106. Powell, C.M., Li, Z.X., McElhinny, M.W., Meert, J.G. and Park, J.K., 1993. Paleomagnetic
1000 constraints on timing of the Neoproterozoic breakup of Rodinia and the Cambrian formation of
1001 Gondwana. *Geology*, 21(10), pp.889-892.
- 1002 107. Powell, C.M. and Pisarevsky, S.A., 2002. Late Neoproterozoic assembly of east Gondwana.
1003 *Geology*, 30(1), pp.3-6.
- 1004 108. Preiss, W.V., 2000. The Adelaide Geosyncline of South Australia and its significance in
1005 Neoproterozoic continental reconstruction. *Precambrian Research*, 100(1), pp.21-63.
- 1006 109. Ratcliff, J.T., Bercovici, D., Schubert, G. and Kroenke, L.W., 1998. Mantle plume heads and
1007 the initiation of plate tectonic reorganizations. *Earth and Planetary Science Letters*, 156(3), pp.195-207.
- 1008 110. Rainbird, R.H., Jefferson, C.W. and Young, G.M., 1996. The early Neoproterozoic
1009 sedimentary Succession B of northwestern Laurentia: Correlations and paleogeographic significance.
1010 *Geological Society of America Bulletin*, 108(4), pp.454-470.

- 1011 111. Santosh, M., 2010. Supercontinent tectonics and biogeochemical cycle: a matter of 'life and
1012 death'. *Geoscience Frontiers*, 1(1), pp.21-30.
- 1013 112. Schmidt, P.W., 2014. A review of Precambrian palaeomagnetism of Australia:
1014 Palaeogeography, supercontinents, glaciations and true polar wander. *Gondwana Research*, 25(3),
1015 pp.1164-1185.
- 1016 113. Schmidt, P.W. and Williams, G.E., 1995. The Neoproterozoic climatic paradox: Equatorial
1017 palaeolatitude for Marinoan glaciation near sea level in South Australia. *Earth and Planetary Science
1018 Letters*, 134(1), pp.107-124.
- 1019 114. Schmidt, P.W. and Williams, G.E., 1996. Palaeomagnetism of the ejecta-bearing Bunyeroo
1020 Formation, late Neoproterozoic, Adelaide fold belt, and the age of the Acraman impact. *Earth and
1021 Planetary Science Letters*, 144(3), pp.347-357.
- 1022 115. Schmidt, P.W. and Williams, G.E., 2013. Anisotropy of thermoremanent magnetisation of
1023 Cryogenian glaciogenic and Ediacaran red beds, South Australia: Neoproterozoic apparent or true
1024 polar wander?. *Global and planetary change*, 110, pp.289-301.
- 1025 116. Schmidt, P.W., Williams, G.E., Camacho, A. and Lee, J.K., 2006. Assembly of Proterozoic
1026 Australia: implications of a revised pole for the ~ 1070 Ma Alcurra Dyke Swarm, central Australia.
1027 *Geophysical Journal International*, 167(2), pp.626-634.
- 1028 117. Schmidt, P.W., Williams, G.E. and McWilliams, M.O., 2009. Palaeomagnetism and
1029 magnetic anisotropy of late Neoproterozoic strata, South Australia: Implications for the
1030 palaeolatitude of late Cryogenian glaciation, cap carbonate and the Ediacaran System. *Precambrian
1031 Research*, 174(1), pp.35-52.
- 1032 118. Sears, J.W. and Price, R.A., 2000. New look at the Siberian connection: No SWEAT.
1033 *Geology*, 28(5), pp.423-426.
- 1034 119. Seton, M., Flament, N., Whittaker, J., Müller, R.D., Gurnis, M. and Bower, D.J., 2015.
1035 Ridge subduction sparked reorganization of the Pacific plate-mantle system 60–50 million years ago.
1036 *Geophysical Research Letters*, 42(6), pp.1732-1740.

- 1037 120. Seton, M., Müller, R.D., Zahirovic, S., Gaina, C., Torsvik, T., Shephard, G., Talsma, A.,
1038 Gurnis, M., Turner, M., Maus, S. and Chandler, M., 2012. Global continental and ocean basin
1039 reconstructions since 200 Ma. *Earth-Science Reviews*, 113(3), pp.212-270.
- 1040 121. Sohl, L.E., Christie-Blick, N. and Kent, D.V., 1999. Paleomagnetic polarity reversals in
1041 Marinoan (ca. 600 Ma) glacial deposits of Australia: implications for the duration of low-latitude
1042 glaciation in Neoproterozoic time. *Geological Society of America Bulletin*, 111(8), pp.1120-1139.
- 1043 122. Squire, R.J., Campbell, I.H., Allen, C.M. and Wilson, C.J., 2006. Did the Transgondwanan
1044 Supermountain trigger the explosive radiation of animals on Earth?. *Earth and Planetary Science Letters*,
1045 250(1), pp.116-133.
- 1046 123. Steinberger, B., Sutherland, R. and O'Connell, R.J., 2004. Prediction of Emperor-Hawaii
1047 seamount locations from a revised model of global plate motion and mantle flow. *Nature*, 430(6996),
1048 pp.167-173.
- 1049 124. Swanson-Hysell, N.L., Maloof, A.C., Kirschvink, J.L., Evans, D.A., Halverson, G.P. and
1050 Hurtgen, M.T., 2012. Constraints on Neoproterozoic paleogeography and Paleozoic orogenesis from
1051 paleomagnetic records of the Bitter Springs Formation, Amadeus Basin, central Australia. *American*
1052 *Journal of Science*, 312(8), pp.817-884.
- 1053 125. Torsvik, T.H., Ashwal, L.D., Tucker, R.D. and Eide, E.A., 2001a. Neoproterozoic
1054 geochronology and palaeogeography of the Seychelles microcontinent: the India link. *Precambrian*
1055 *Research*, 110(1), pp.47-59.
- 1056 126. Torsvik, T.H., Carter, L.M., Ashwal, L.D., Bhushan, S.K., Pandit, M.K. and Jamtveit, B.,
1057 2001b. Rodinia refined or obscured: palaeomagnetism of the Malani igneous suite (NW India).
1058 *Precambrian Research*, 108(3), pp.319-333.
- 1059 127. Torsvik, T.H. and Cocks, L.R.M., 2013. New global palaeogeographical reconstructions for
1060 the Early Palaeozoic and their generation. *Geological Society, London, Memoirs*, 38(1), pp.5-24.
- 1061 128. Torsvik, T.H., Steinberger, B., Cocks, L.R.M. and Burke, K., 2008. Longitude: linking
1062 Earth's ancient surface to its deep interior. *Earth and Planetary Science Letters*, 276(3), pp.273-282.

- 1063 129. Torsvik, T.H., Van der Voo, R., Preeden, U., Mac Niocaill, C., Steinberger, B., Doubrovine,
1064 P.V., van Hinsbergen, D.J., Domeier, M., Gaina, C., Tohver, E. and Meert, J.G., 2012. Phanerozoic
1065 polar wander, palaeogeography and dynamics. *Earth-Science Reviews*, 114(3), pp.325-368.
- 1066 130. Van der Meer, D.G., Spakman, W., Van Hinsbergen, D.J., Amaru, M.L. and Torsvik, T.H.,
1067 2010. Towards absolute plate motions constrained by lower-mantle slab remnants. *Nature Geoscience*,
1068 3(1), pp.36-40.
- 1069 131. Van der Voo, R., Spakman, W. and Bijwaard, H., 1999. Tethyan subducted slabs under
1070 India. *Earth and Planetary Science Letters*, 171(1), pp.7-20.
- 1071 132. van Hinsbergen, D.J., Steinberger, B., Doubrovine, P.V. and Gassmüller, R., 2011.
1072 Acceleration and deceleration of India-Asia convergence since the Cretaceous: Roles of mantle
1073 plumes and continental collision. *Journal of Geophysical Research: Solid Earth*, 116(B6).
- 1074
- 1075 133. Walter, M.R., Grey, K., Williams, I.R. and Calver, C.R., 1994. Stratigraphy of the
1076 Neoproterozoic to early Palaeozoic Savory basin, western Australia, and correlation with the
1077 Amadeus and Officer basins. *Australian Journal of Earth Sciences*, 41(6), pp.533-546.
- 1078 134. Wang, W. and Zhou, M.F., 2012. Sedimentary records of the Yangtze Block (South China)
1079 and their correlation with equivalent Neoproterozoic sequences on adjacent continents. *Sedimentary*
1080 *Geology*, 265, pp.126-142.
- 1081 135. Weil, A.B., Geissman, J.W. and Van der Voo, R., 2004. Paleomagnetism of the
1082 Neoproterozoic Chuar Group, Grand Canyon Supergroup, Arizona: implications for Laurentia's
1083 Neoproterozoic APWP and Rodinia break-up. *Precambrian Research*, 129(1), pp.71-92.
- 1084 136. Wessel, P., Matthews, K.J., Müller, R.D., Mazzoni, A., Whittaker, J.M., Myhill, R. and
1085 Chandler, M.T., 2015. Semiautomatic fracture zone tracking. *Geochemistry, Geophysics, Geosystems*,
1086 16(7), pp.2462-2472.
- 1087 137. Wessel, P. and Müller, R.D., 2015 6.02 - Plate Tectonics, in: Schubert, G. (Ed.), *Treatise on*
1088 *Geophysics* (Second Edition), Elsevier, Oxford, pp. 45-93

- 1089 138. Whittaker, J.M., Müller, R.D., Leitchkov, G., Stagg, H., Sdrolias, M., Gaina, C. and
1090 Goncharov, A., 2007. Major Australian-Antarctic plate reorganization at Hawaiian-Emperor bend
1091 time. *Science*, 318(5847), pp.83-86.
- 1092 139. Williams, G.E., Gostin, V.A., McKirdy, D.M. and Preiss, W.V., 2008. The Elatina
1093 glaciation, late Cryogenian (Marinoan Epoch), South Australia: sedimentary facies and
1094 palaeoenvironments. *Precambrian Research*, 163(3), pp.307-331.
- 1095 140. Wingate, M.T. and Giddings, J.W., 2000. Age and palaeomagnetism of the Mundine Well
1096 dyke swarm, Western Australia: implications for an Australia-Laurentia connection at 755 Ma.
1097 *Precambrian Research*, 100(1), pp.335-357.
- 1098 141. Wingate, M.T., Pisarevsky, S.A. and Evans, D.A., 2002. Rodinia connections between
1099 Australia and Laurentia: no SWEAT, no AUSWUS?. *Terra Nova*, 14(2), pp.121-128.
- 1100 142. Wingate, M.T., Pisarevsky, S.A. and De Waele, B., 2010. Paleomagnetism of the 765 Ma
1101 Luakela volcanics in Northwest Zambia and implications for Neoproterozoic positions of the Congo
1102 Craton. *American Journal of Science*, 310(10), pp.1333-1344.
- 1103 143. Wit, M.J., Bowring, S.A., Ashwal, L.D., Randrianasolo, L.G., Morel, V.P. and Rabeloson,
1104 R.A., 2001. Age and tectonic evolution of Neoproterozoic ductile shear zones in southwestern
1105 Madagascar, with implications for Gondwana studies. *Tectonics*, 20(1), pp.1-45.
- 1106 144. Yellappa, T., Chetty, T.R.K., Tsunogae, T. and Santosh, M., 2010. The Manamedu
1107 Complex: Geochemical constraints on Neoproterozoic suprasubduction zone ophiolite formation
1108 within the Gondwana suture in southern India. *Journal of Geodynamics*, 50(3), pp.268-285.
- 1109 145. Yin, A., Dubey, C.S., Webb, A.A.G., Kelty, T.K., Grove, M., Gehrels, G.E. and Burgess,
1110 W.P., 2010. Geologic correlation of the Himalayan orogen and Indian craton: Part 1. Structural
1111 geology, U-Pb zircon geochronology, and tectonic evolution of the Shillong Plateau and its
1112 neighboring regions in NE India. *Geological Society of America Bulletin*, 122(3-4), pp.336-359.
- 1113 146. Young, G.M., 1981. Upper Proterozoic supracrustal rocks of North America: a brief review.
1114 *Precambrian Research*, 15(3), pp.305-330.
- 1115 147. Young, G.M., Jefferson, C.W., Delaney, G.D. and Yeo, G.M., 1979. Middle and late
1116 Proterozoic evolution of the northern Canadian Cordillera and Shield. *Geology*, 7(3), pp.125-128.

- 1117 148. Zahirovic, S., Müller, R.D., Seton, M. and Flament, N., 2015. Tectonic speed limits from
1118 plate kinematic reconstructions. *Earth and Planetary Science Letters*, 418, pp.40-52.
- 1119 149. Zahirovic, S., Seton, M. and Müller, R.D., 2014. The Cretaceous and Cenozoic tectonic
1120 evolution of Southeast Asia. *Solid Earth*, 5(1), p.227.
- 1121 150. Zhao, J.H., Zhou, M.F., Yan, D.P., Zheng, J.P. and Li, J.W., 2011. Reappraisal of the ages
1122 of Neoproterozoic strata in South China: no connection with the Grenvillian orogeny. *Geology*, 39(4),
1123 pp.299-302.